Traditional Indian Medicine

Medicinal plant-based saponins targeting COVID-19 M^{pro} in silico

Mohd Rehan[1], Shafiullah[1*]

[1]Department of Chemistry, Aligarh Muslim University, Aligarh 202002, Uttar Pradesh, India.

*Corresponding to: Shafiullah. Department of Chemistry, Aligarh Muslim Unversity, Street, Collectorate and Gantha Ghar Road, Aligarh, District Aligarh 202002, Uttar Pradesh, India. E-mail: shafiullah1966@gmail.com.

Highlights

Approximately 34 saponins are more effective on COVID-19 M^{pro} than hydroxychloroquine, chloroquine, and nelfinavir. 13 saponins exhibit high potency against COVID-19 M^{pro} due to more binding energies than 10 kcal/mol.

Tradition

Medicinal plants have been used for health care since ancient times worldwide in the traditional system of medicine such as Unani, Siddha, Ayurveda, and traditional Tibetan and Chinese medicine. Jiaogulan (*Gynostemma pentaphyllum*) is the source of the dammarane-type saponins, which was described in 1406 C.E. by Zhu Xiao in the ancient Chinese medicine classics *Materia Medica for Famine* as a survival food. Renshen (*Panax ginseng*) which was first recorded in *Shennong's Classic of Materia Medica* written between about 200 C.E. and 250 C.E. is a big source of saponins, which was used for medicinal purposes over 3,000 years ago. Various types of saponins such as hopane, lupane, and oleanane have been isolated from many parts such as leaves, roots, barks, stems, and rhizomes of various herbs. The main advantage of saponins is to protect plants against various pathogen attacks.

ARTICLE
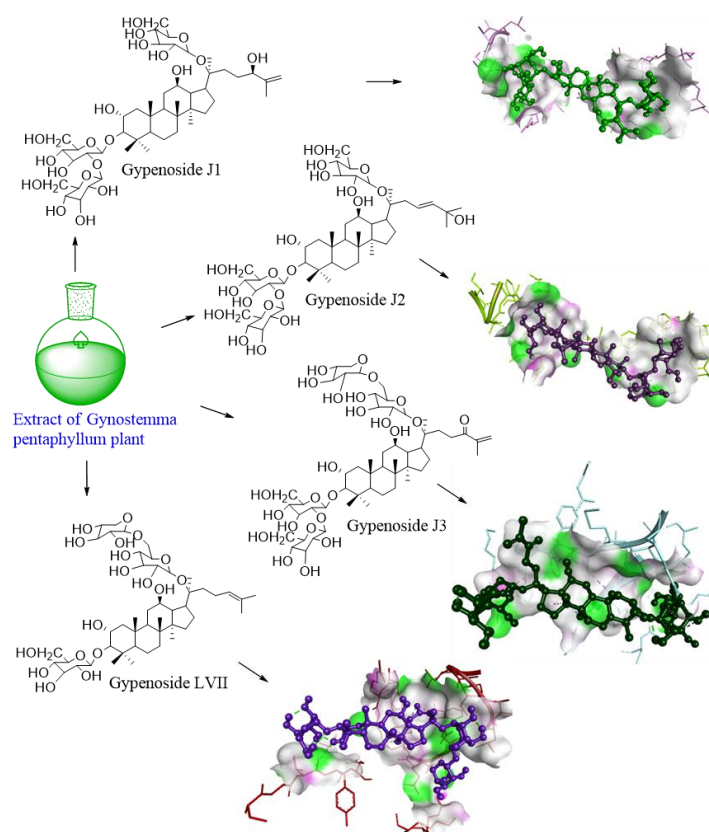
Abstract

Background: Recently, the Chinese scientists Liu et al. demonstrated a crystallized form of severe acute respiratory syndrome coronavirus-2 main protease (M^{pro}), the best target of the drug, which was published in *Nature* in June 2020. Many components of herbs are determined as the potential inhibitors of coronavirus disease 2019 (COVID-19) M^{pro} such as quercetin, cirsimaritin, hispidulin, and flavonoids. **Methods:** Library of herb-based bioactive saponins are analyzed with 6LU7 M^{pro} using AutoDock tools 1.5.6, BIOVIA Discovery Studio 2017 R2, Chimera 1.13.1, and AutoDock Vina to evaluate their potency against COVID-19 M^{pro}. The conventional Western medicines, including hydroxychloroquine, chloroquine and nelfinavir, are used as positive controls for comparison. **Results:** Binding energies of 60 saponins with 6LU7 M^{pro} are obtained in which approximately 34 saponins are more effective on COVID-19 M^{pro} than hydroxychloroquine, chloroquine, and nelfinavir. 13 saponins exhibit high potency against COVID-19 M^{pro} due to more binding energies than 10 kcal/mol. **Conclusion:** Further research on all effective saponins is needed to evaluate the real medicinal potential against COVID-19.

Keywords: Saponins, COVID-19, Molecular docking, 6LU7, M^{pro}, SARS-CoV-2

Background

Coronavirus disease 2019 (COVID-19) is a respiratory infectious disease, first identified in Wuhan, China, and spread globally [1]. This novel type of coronavirus is now known as severe acute respiratory syndrome coronavirus-2 (SARS-CoV-2) [2]. Symptoms of this virus disease include difficulty in breathing, fever, dry cough, dyspnea, fatigue, and frost-glass-like symptoms in the lungs [3]. According to World Health Organization situation report 170, a total of 5,39,906 deaths and 1,16,69,259 confirmed cases have been reported in more than 210 countries from COVID-19 till July 8, 2020 [4]. There are no approved drugs or vaccines available for the treatment of infected humans; on the other hand, patients are being treated by a few antiviral strategies [5]. So, this disease is considered a serious problem in various countries and the infection is increasing day by day. Thus, potent antiviral drugs are needed for the treatment of COVID-19.

SARS-CoV-2 was isolated by Chinese scientists and genome sequence closely related to bat-derived SARS-like coronavirus [6]. The crystal structure of COVID-19 main protease (M^{pro}) is a good drug target protein for the inhibition of SARS-Cov-2 replication and is demonstrated by a Chinese researcher. In recent studies, Michael acceptor inhibitor (named N3) and flavonoids are potential inhibitors, which target COVID-19 M^{pro} (PDB ID: 6LU7) in silico [7–8]. According to Sekiou O et al. (2020), quercetin, cirsimaritin, and hispidulin are better inhibitors against COVID-19 M^{pro} than hydroxychloroquine [9]. Zhang et al. determined the crystal structure of M^{pro} in coronavirus, developed a compound into a potent inhibitor, and obtained a structure with the inhibitor bound [10]. Thus, M^{pro} has a high potential for drugs targeting the treatment of COVID-19 by inhibition of the viral polypeptide cleavage.

In this study, we have screened a diverse type of saponins against COVID-19 M^{pro}. Various types of saponins such as hopane, lupane, oleanane, ursane, steroids, spirostanol, furastanol, dammarane, and cycloartane have been isolated from many parts of various herbs such as leaves, root, barks, stems, and rhizomes [11]. These parts have been used for health care since ancient times worldwide in the traditional system of medicine such as Unani, Siddha, Ayurveda, and traditional Tibetan and Chinese medicine [12–13]. Renshen (*Panax ginseng*), first recorded in *Shennong's Classic of Materia Medica* written between about 200 C.E. and 250 C.E., is a big source of saponins, which was used for medicinal purposes over 3,000 years ago [14]. Jiaogulan (*Gynostemma pentaphyllum*) is the source of dammarane-type saponins, which was described in 1406 C.E. by Zhu Xiao in the book *Materia Medica for Famine* as a survival food [15]. The main advantage of saponins is to protect plants against various pathogen attacks [16]. Saponins play a key role in enhancing both cell-mediated and humoral immune responses to antigens and they were found to show antiviral activity against both RNA and DNA viruses [17–18]. When saponins are added to a vaccine, they increase antigen-specific antibody production and induce a strong cytotoxic T-lymphocyte response [19–21].

Computational screening studies play a key role in antiviral drug discovery and save resources in terms of money as well as time [22]. In this study, we have screened a library of saponins against the main protease of COVID-19 using molecular docking and identified the potential of medicinal plant-based saponins against COVID-19 in clinical trials.

Materials and methods

Preparation of target protein (6LU7) receptor

The three-dimensional crystal structure of the target protein (COVID-19 M^{pro}) was downloaded from the RCSB protein data bank (https://www.rcsb.org) (PDB ID: 6LU7, resolution: 2.16 A°) [23]. To stabilize the kinases structures, the ligands and water molecules were removed by BIOVIA Discovery Studio 2017 R2 software. The Gasteiger charges and hydrogenating atoms were added to the protein and then converted into a proper readable file format (PDBQT) by AutoDock tool 1.5.6 software and AutoDock Vina software (http://vina.scripps.edu/). A grid box on active residues of protein was generated with grid dimension, grid spacing (1 A°), and grid center by proximity to the ligand. The exhaustiveness was set at 50 and binding energy was predicted with the Lamarckian genetic algorithm and AutoDock Vina software.

Preparation of ligands (several type of saponins)

All ligand structures (several types of saponins) which were used in docking experiments such as ginsenoside Rg12, hederagenin-3-O-β-D-glucopyranosyl-(1 → 3)-α-L-rhamnopyranosyl-(1 → 2)-α-L-rhamnopyranosyl-(1 → 2)-α-L-arabinopyranoside, and TPG5 (3-O-α-L-rhamnopyranosyl asiatic acid (TPG1), acankoreoside A, gypenoside J2, paristenoside B, cyclocarioside Q, gypenoside J3, paristenoside A, etc.) were performed by Chem 3D Pro 12.0.2.1076 software. All ligands (structure of saponins) were converted to energetically most stable structure using energy minimization and stored in a PDB format file. Hydrogenating atoms and chosen torsion were added to PDB format file and finally stored and saved in a PDBQT format file.
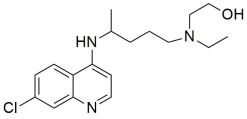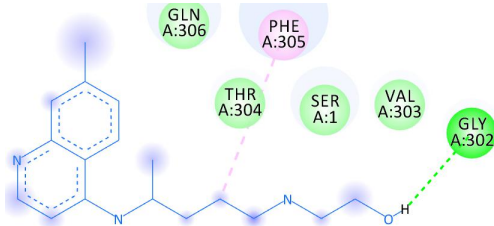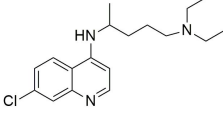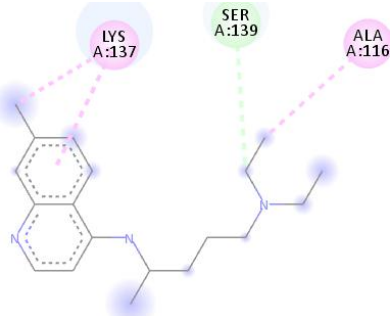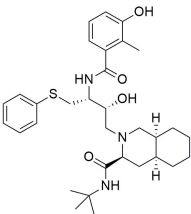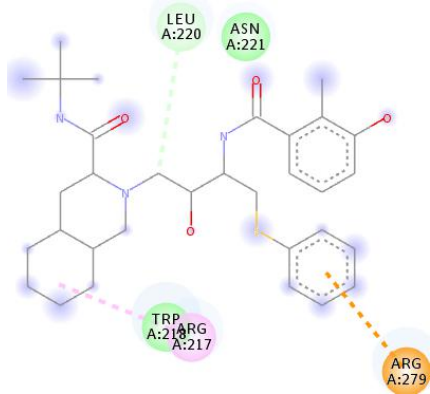
Molecular docking

All experiments (docking calculation) of saponin structures with COVID-19 M^{pro} were performed by AutoDock Vina software because it offers more

accuracy in protein-ligand interaction. Three conventional medicines, including hydroxychloroquine, chloroquine and nelfinavir, were screened with COVID-19 M^pro in silico for known binding energy. These drugs have potential and have been studied experimentally for the treatment of COVID-19 [24]. Using AutoDock Vina software, the binding energies of 40 active saponins with COVID-19 M^pro were obtained in a range from −11.9 to −6.7 kcal/mol. The final visualization of the docked structure was performed using BIOVIA Discovery Studio 2017 R2 software. Hydroxychloroquine, chloroquine, and nelfinavir are being used for the treatment of COVID-19, malaria, and human immunodeficiency virus and utilized as a positive control.

Table 1 Potential drugs of coronavirus disease 2019 main protease inhibitors

Entry	Structure/name	Interaction of structure with 4LU7	Docking affinity (kcal/mol)	Amino acid residue
1	Hydroxychloroquine		−4.6	Gly-302; Phe-305
2	Chloroquine		−5.6	Ser-139; Ala-116; Lys-137
3	Nelfinavir		−7.6	Leu-220; Arg-217; Arg-279
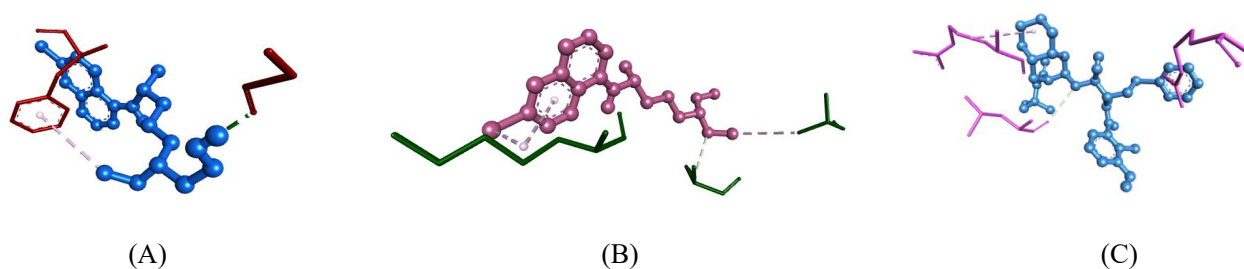
Figure 1 (A) Molecular docking of hydroxychloroquine (ball and stick), (B) chloroquine (ball and stick), and (C) nelfinavir (ball and stick) with active site of coronavirus disease 2019 main protease (PDB: 6LU7).

Results

Binding energy of hydroxychloroquine, chloroquine, and nelfinavir

Docking studies of hydroxychloroquine drug with 6LU7 show binding energy of −4.6 kcal/mol. Hydrogen and pi-alkyl hydrophobic binding is displayed with amino acids Gly-302 and Phe-305 (Figure 1(1); Table 1, entry 1). Chloroquine forms hydrogen and hydrophobic interaction with amino acids Ser-139, Ala-116, and Lys-137 and shows binding energy of −5.6 kcal/mol (Figure 1 (2); Table 1, entry 2). Nelfinavir forms pi-anion, hydrogen, and alkyl/pi-alkyl hydrophobic interaction with amino acids Glu-14, Gly-11, Lys-12, Lys-97, and Pro-99 and shows binding energy of −6.4 kcal/mol (Figure 1 (3); Table 1, entry 3). These three drugs are used as a positive control.

Binding energy of saponins

60 saponin are screened with 6LU7 M^{pro} for the known best inhibitory target of COVID-19. From screening, 34 saponins show more binding energy than chloroquine, hydroxychloroquine, and nelfinavir, in which the binding energy of 13 saponins is more than 10 kcal/mol.

3-O-β-D-Xylopyranosyl-6-O-β-D-glucopyranosyl-1 6-O-β-D-glucopyranosyl-3β,6α,16β,24(S)-25-pentahyd roxycycloartane exhibits high binding energy of −11.9 kcal/mol. Interaction of this saponin with 6LU7 shows five hydrogen bonds with amino acids Arg-4, Gln-127, Gln-127, Ser-139, and Glu-290, one pi-sigma bond with Tyr-126, and an alkyl/pi-alkyl hydrophobic bond with Lys-5 and Tyr-126 (Figure 2 (1); Table 2, entry 1). Ginsenoside Rg12 is a dammarane-type saponin which forms two hydrogen bonds with Thr-199 and Ala-285, one carbon-hydrogen bond with Asp-197, and a hydrophobic bond with Leu-272, Leu-286, and Leu-287 (Figure 2 (2); Table 2, entry 2). TPG1 is an oleanane-type saponin which forms one hydrogen bond with Thr-199 and a hydrophobic bond with Lys-137 and Leu-286 (Figure 2 (3); Table 2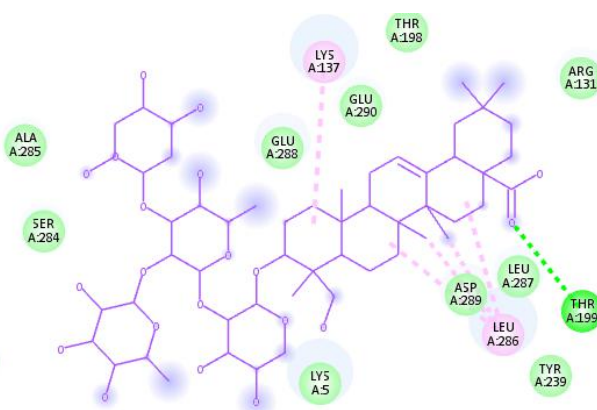, entry 3). (23S,24S)-21-Hydroxymethyl-24-{[O-β-d-glucopyran osyl-(1→4)-β-dfucop-yranosyl]oxy}-3β,23-dihydroxys pirosta-5,25(27)-diene-1β-yl O-(α-L-rhamnopyranosyl)-(1→2)-O-[β-d-xylopyranosyl-(1→3)-α-L-arabinopyr anoside exhibits binding energy of −10.7 kcal/mol. It is a steroidal-type saponin which forms two hydrogen bonds with Ser-10 and Val-125 (Figure 2 (4); Table 2, entry 4). 3β-O-[α-L-Rhamnopyranosyl-(1→2)-β-D-glucopyranosyl-(1→2)-β-D-glucuronopyranosyl] betulinic acid 28-O-[α-L-rhamnopyranosyl-(1→4)-β-D-glucopyranoside] is a lupane-type saponin which forms one conventional hydrogen bond with Glu-288, a carbon-hydrogen bond with Met-6 and Lys-137, an alkyl/pi-alkyl hydrophobic bond with Ala-7, Tyr-126, and Cys-128, and one violation bond with Val-125 (Figure 2 (5); Table 2, entry 5). Acankoreoside A is found in the leaves of *Acanthopanax gracilistylus* plant which forms five hydrogen bonds with Gln-127, Lys-137, Gly-283, Glu-288, and Glu-290 and a hydrophobic bond with Lys-5 (Figure 2 (6); Table 2, entry 6). Gypenoside J2 is a dammarane-type saponin which forms three hydrogen bonds with Ser-139, Ser-123, and Ser-139 and an alkyl/pi-alkyl hydrophobic bond with Lys-5 and Tyr-126 (Figure 2 (7); Table 2, entry 7). Paristenoside B is a spirostanol-type saponin which forms three conventional hydrogen bonds with Ser-10, Glu-14, and Ser-139, one carbon-hydrogen bond with Gly-124, and an alkyl/pi-alkyl hydrogen bond with Ala-116 and Tyr-126 (Figure 2 (8); Table 2, entry 8). TPG2 is an oleanane-type saponin which exhibits binding energy of −10.2 kcal/mol (Figure 2 (9); Table 2, entry 9). Cyclocarioside Q is found in the leaves which exhibits binding energy of −10.2 kcal/mol (Figure 2 (10); Table 2, entry 10). Gypenoside J1 forms seven hydrogen bonds with Phe-3, Ser-123, Gly-283, Ser-139, Phe-3, Ser-123, and Arg-4 and an alkyl/pi-alkyl hydrophobic bond with Lys-5 and Tyr-126 (Figure 2 (11); Table 2, entry 11). Gypenoside J3 exhibits binding energy of −10.2 kcal/mol which was reported from *Gynostemma pentaphyllum* plant (Figure 2 (12); Table 2, entry 12). Paristenoside A is found in *Paris polyphylla* plant which exhibits binding energy of −10.0 kcal/mol (Figure 2 (13); Table 2, entry 13).
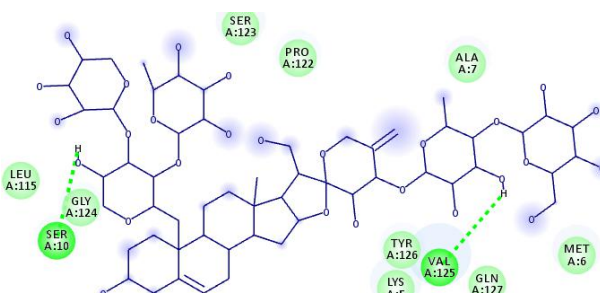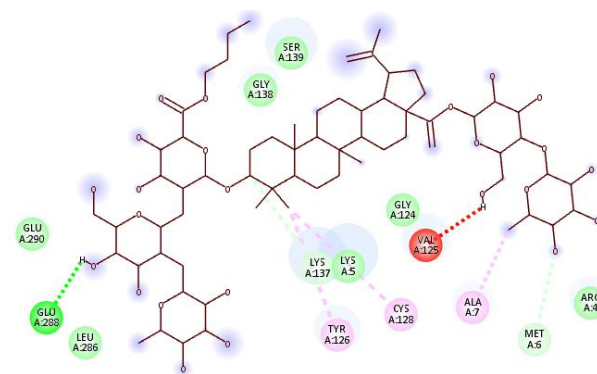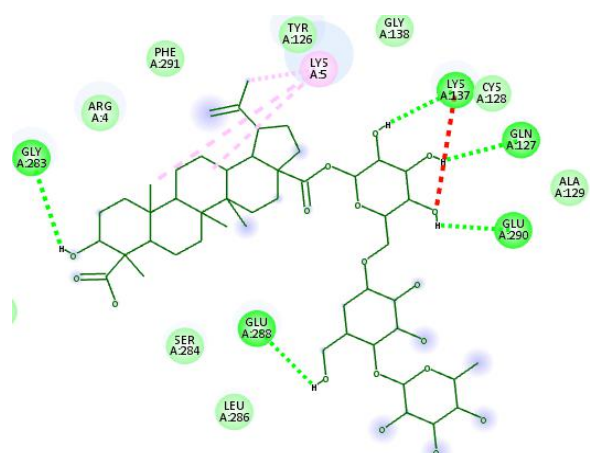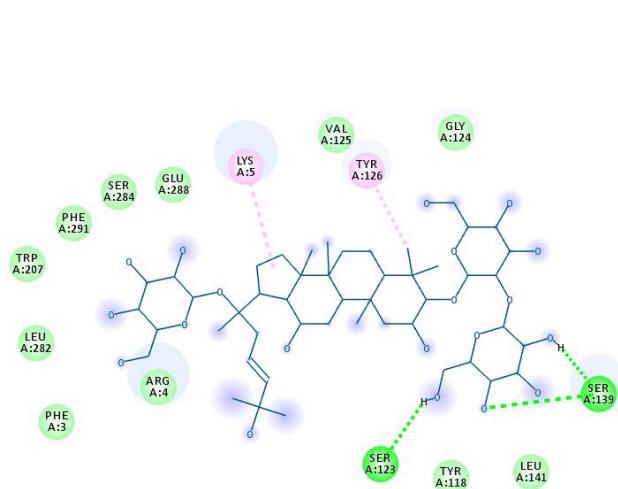
(1)

(2)
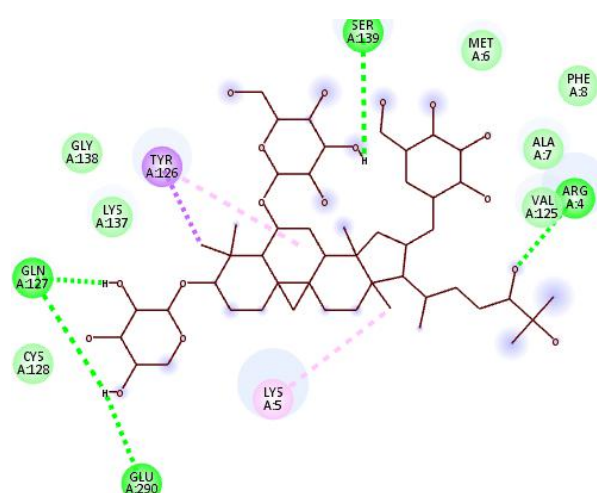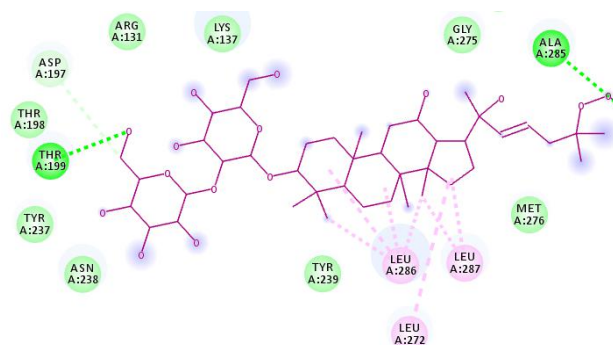
(3)

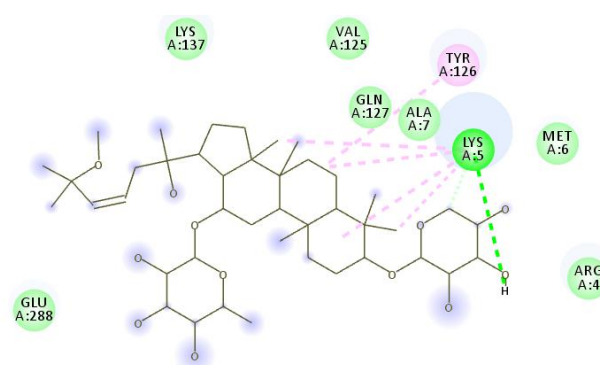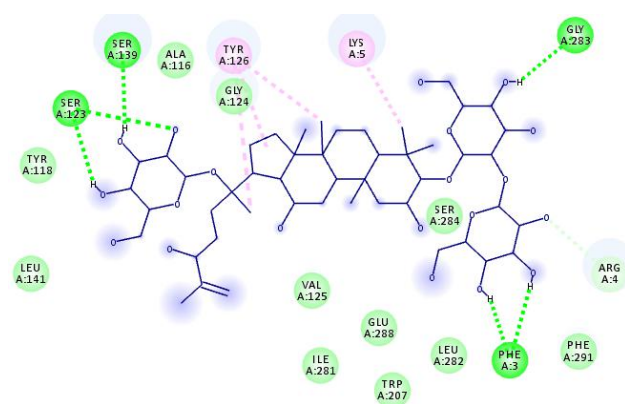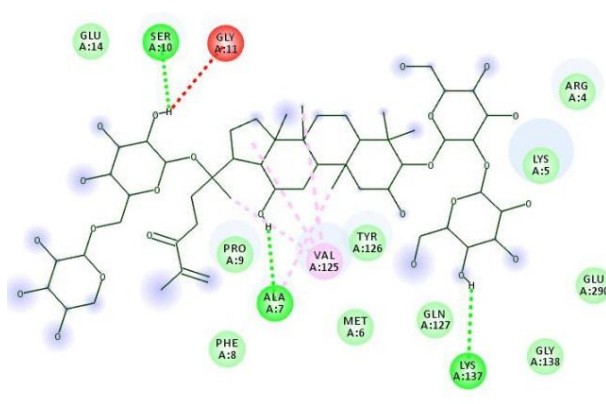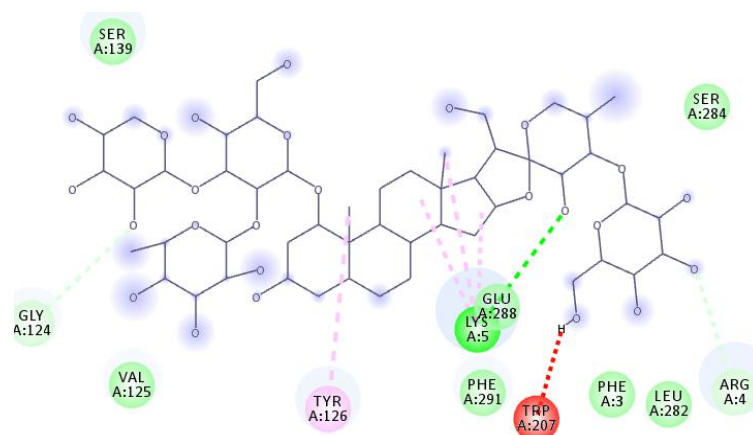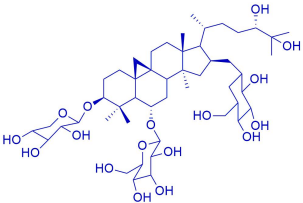(4)

(5)

(6)

(7)
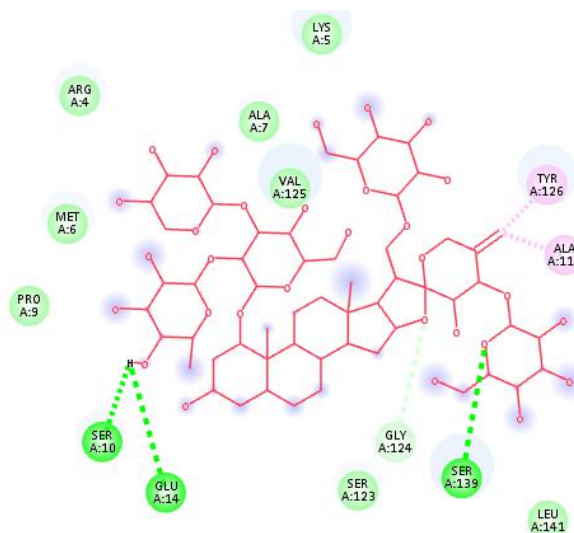
(8)
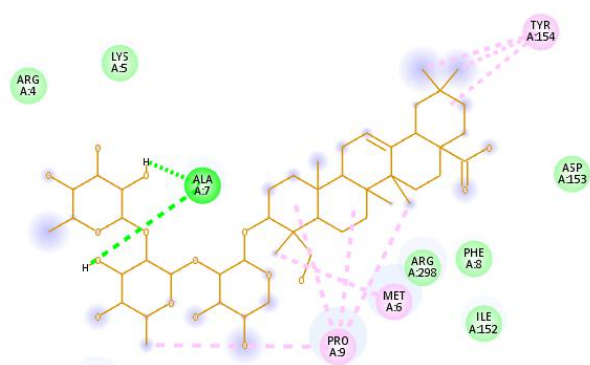
(9)

(10)

(11)

(12)

(13)

Figure 2 Binding interaction of coronavirus disease 2019 main protease with saponin structures. (1) 3-O-β-D-xylopyranosyl-6-O-β-D-glucopyranosyl-16-O-β-D-glucopyranosyl-3β,6α,16β,24(S)-25-pentahydroxycycl oartane, (2) ginsenoside Rg12, (3) TPG1, **(**4) (23S,24S)-21-hydroxymethyl-24-{[O-β-d-glucopyranosyl-(1→4)-β-dfucop-yranosyl]oxy}-3β,23-dihydroxyspirosta-5,25(27)-diene-1β-yl O-(α-L-rhamnopyranosyl)-(1→2)-O-[β-d-xyl opyranosyl-(1→3)-α-L-arabinopyranoside, (5) 3β-O-[α-L-rhamnopyranosyl-(1→2)-β-D-glucopyranosyl-(1→2)-β-D-glucuronopyranosyl] betulinic acid 28-O-[α-L-rhamnopyranosyl-(1→4)-β-D-glucopyranoside], (6) acankoreoside A, (7) gypenoside J2, (8) paristenoside B, (9) TPG2, (10) cyclocarioside Q, (11) gypenoside J1, (12) gypenoside J3, and (13) paristenoside A.

Table 2 More binding energies from 10 kcal/mol and high interaction of 13 saponins against coronavirus disease 2019 main protease
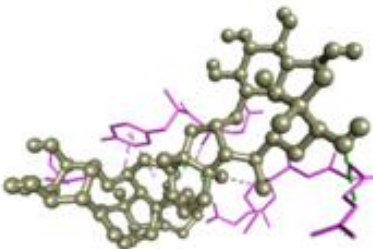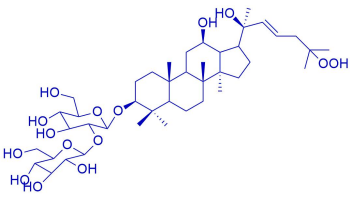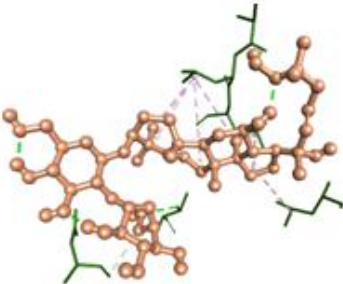
Entry	Structure/name	Interaction of structure with 4LU7	Docking affinity (kcal/mol)	Amino acid residue
1	3-O-β-D-Xylopyranosyl-6-O-β-D-glucopyranosyl-16-O-β-D-glucopyranosyl-3β,6α,16β,24(S)-25-pentahydroxycycloartane		−11.9	Arg-4; Gln-127; Gln-127; Ser-139; Glu-290; Tyr-126; Lys-5; Tyr-126
2	Ginsenoside Rg12		−10.9	Thr-199; Ala-285; Asp-197; Leu-272; Leu-286; Leu-287

Table 2 More binding energies from 10 kcal/mol and high interaction of 13 saponins against coronavirus disease 2019 main protease (*Continued*)
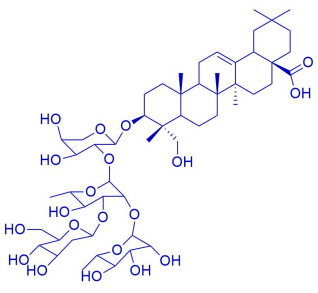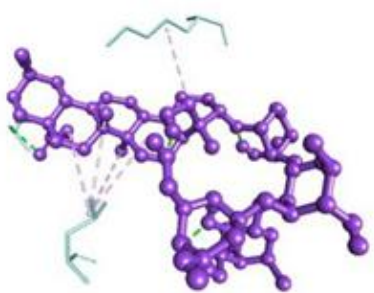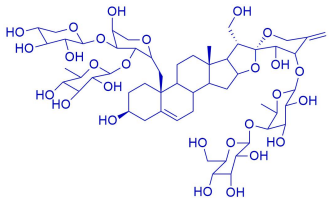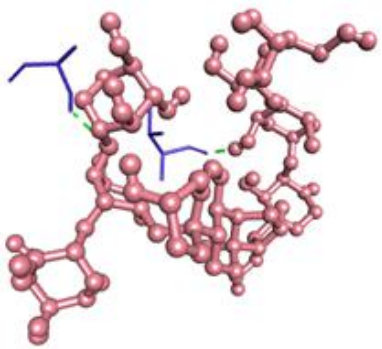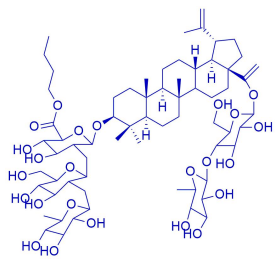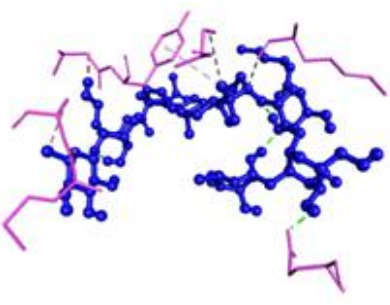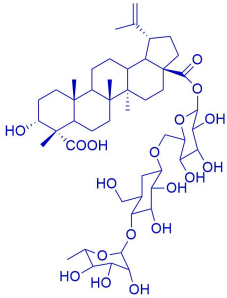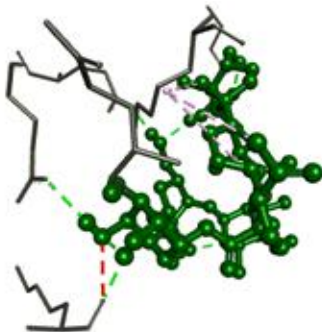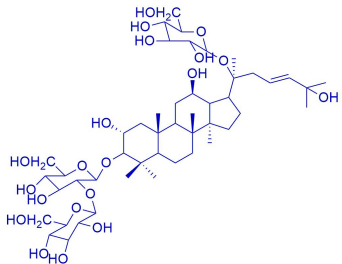
Entry	Structure/name	Interaction of structure with 4LU7	Docking affinity (kcal/mol)	Amino acid residue
3	TPG1		−10.9	Thr-199; Lys-137; Leu-286
4	(23S,24S)-21-Hydroxymethyl-24-{[O-β-d-glucopyranosyl-(1→4)-β-dfucop-yranosyl]oxy}-3β,23-dihydroxyspirosta-5,25(27)-diene-1β-ylO-(α-L-rhamno pyranosyl)-(1→2)-O-[β-d-xylo pyranosyl-(1→3)-α-L-arabino pyranoside		−10.7	Ser-10; Val-125
5	3β-O-[α-L-Rhamnopyranosyl-(1 → 2)-β-D-glucopyranosyl-(1→2)-β-D-glucuronopyranosyl] betulinic acid 28-O-[α-L-rhamnopyranosyl-(1→4)-β-D-glucopyranoside]		−10.5	Glu-288; Met-6; Lys-137; Ala-7; Tyr-126; Cys-128

Table 2 More binding energies from 10 kcal/mol and high interaction of 13 saponins against coronavirus disease 2019 main protease (*Continued*)
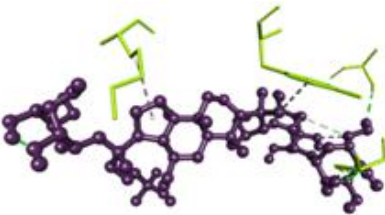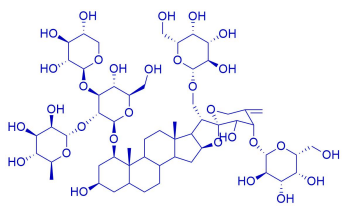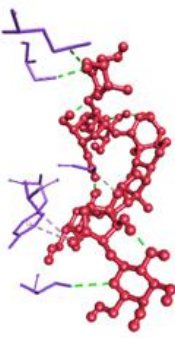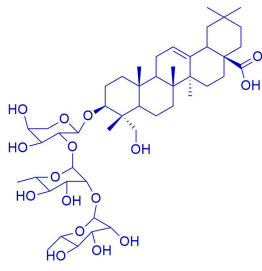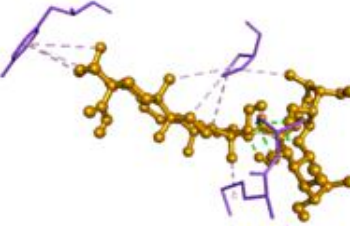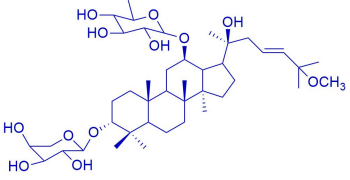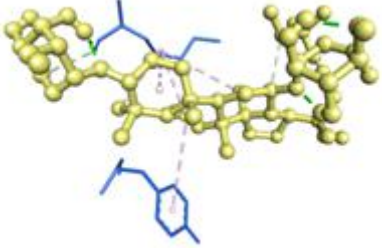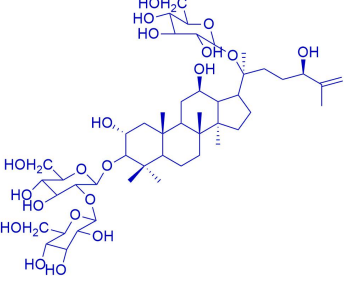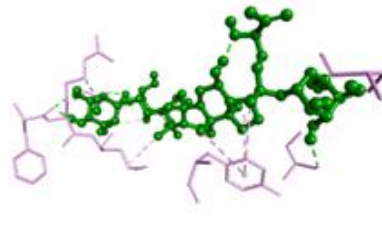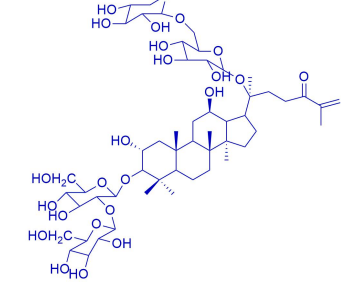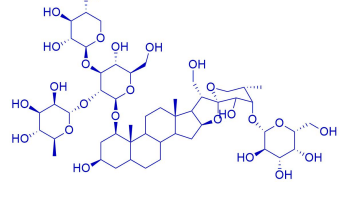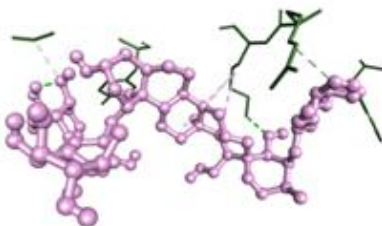
Entry	Structure/name	Interaction of structure with 4LU7	Docking affinity (kcal/mol)	Amino acid residue
6	Acankoreoside A		−10.5	Gln-127; Lys-137; Gly-283; Glu-288; Glu-290; Lys-5
7	Gypenoside J2		−10.4	Ser-139; Ser-123; Ser-139; Lys-5; Tyr-126
8	Paristenoside B		−10.3	Ser-10; Glu-14; Ser-139; Gly-124; Ala-116; Tyr-126
9	TPG2		−10.2	Ala-7; Ala-7; Met-6; Pro-9; Tyr-154

Table 2 More binding energies from 10 kcal/mol and high interaction of 13 saponins against coronavirus disease 2019 main protease (*Continued*)

Entry	Structure/name	Interaction of structure with 4LU7	Docking affinity (kcal/mol)	Amino acid residue
10	Cyclocarioside Q		−10.2	Lys-5; Lys-5; Tyr-126; Lys-5
11	Gypenoside J1		−10.2	Phe-3; Ser-123; Gly-283; Ser-139; Phe-3; Ser-123; Arg-4; Lys-5; Tyr-126
12	Gypenoside J3		−10.2	Ala-7; Ser-10; Lys-137; Val-125; Ala-7
13	Paristenoside A		−10.0	Lys-5; Arg-4; Tyr-126; Lys-5

Molecular docking analysis of 27 saponins with COVID-19 M^{pro} exhibits binding energies in the range from −6.7 to −9.8 kcal/mol. Gypenoside LVII forms two hydrogen bonds with Val-125 and Val-125 and an alkyl/pi-alkyl hydrophobic bond with Lys-5, Trp-207, and Phe-291 (Figure 3 (1); Table 3, entry 1). Smilscobinoside F is found in the rhizome of *Smilax scobinicaulis* plant which forms two hydrogen bonds with Trp-218 and Leu-220 and a hydrophobic bond with Leu-220 (Figure 3 (2); Table 3, entry 2). Glinusopposide L is a hopane-type saponin which forms two conventional hydrogen bonds with Thr-199 and Asp-289, one carbon-hydrogen bond with Leu-287, and an alkyl hydrophobic bond with Leu-286 (Figure 3 (3); Table 3, entry 3). 25-O-Acetylcimigenol-3-O-(3'-O-3-methoxy-3-oxopropionyl)-β-D-xylopyranoside is a cycloartane-type saponin which exhibits binding energy of −8.9 kcal/mol (Figure 3 (4); Table 3, entry 4). Calendustellatoside E forms four hydrogen bonds with Arg-4, Val-125, Gly-283, and Glu-288 and a pi-alkyl hydrophobic bond with Tyr-126 (Figure 3 (5); Table 3, entry 5). Schekwanglupaside A is a lupane-type saponin which forms two conventional hydrogen bonds with Ser-123 and Ser-139, one carbon-hydrogen bond with Val-125, and a hydrophobic bond with Lys-5, Ala-7, Tyr-126, and Phe-291 (Figure 3 (6); Table 3, entry 6). Gylongiposide I forms one conventional hydrogen bond with Phe-3, four carbon-hydrogen bonds with Gly-2, Phe-3, Arg-4, and Asp-216, and a hydrophobic bond with Val-303 and Phe-305 (Figure 3 (7); Table 3, entry 7). (1S,15R)-1,15,25-Trihydroxy-3-O-β-D-xylopyranosyl-acta-(16S,23R,24R)-16,23;16,24-binoxoside is a cycloartane-type saponin which exhibits binding energy of −8.8 kcal/mol (Figure 3 (8); Table 3, entry 8). 3-O-α-L-Arabinopyranosyl-(1S,24R)-1,24,25-trihydroxy-15-oxo-acta-(16R,23R)-16,23-monoxoside exhibits binding energy of −8.8 kcal/mol (Figure 3 (9); Table 3, entry 9). 9 (R), 19, 22 (S), 24 (R)

Dicyclolanost-3β, 12α, 16β, 17α tetrol-25-one 3-O-β-D-glucopyranosyl-(1→2)-β-D-glucopyranoside is found in aerial parts of *Mussaenda luteola* plant which exhibits binding energy of −8.6 kcal/mol (Figure 3 (10); Table 3, entry 10). TPG3 (Figure 3 (11); Table 3, entry 11), cimiheraclein G (Figure 3 (12); Table 3, entry 12), (20R)-16,21-O-di-(β-D-fucopyranosyl)-24-methyl-cholesta-5,24(28)-diene-3β,7α,16α,21-tetraol (Figure 3 (13); Table 3, entry 13), calendustellatoside D (Figure 3 (14); Table 3, entry 14), 2α,3β,23-trihydroxylup-20(29)-en-28-oic acid 3-O-α-L-arabinopyranoside (Figure 3 (15); Table 3, entry 15), yesanchinoside R$_3$ (Figure 3 (16); Table 3, entry 16), anemarsaponin B (Figure 3 (17); Table 3, entry 17), actein (Figure 3 (18); Table 3, entry 18), glinusopposide M (Figure 3 (19); Table 3, entry 19), schekwanglupaside B (Figure 3 (20); Table 3, entry 20), 3-O-β-D-glucopyranosyl 3α, 11α-dihydroxylup-20(2-en-28-oic acid (Figure 3 (21); Table 3, entry 21), t (Figure 3 (22); Table 3, entry 22), 3β,6β-dihydroxy-7β-((4-hydroxybenzoyl)oxy)-21αH-24-norhopa-4(23),22(29)-diene (Figure 3 (23); Table 3, entry 23), 6β,11α-dihydroxy-7β-((4-hydroxybenzoyl)oxy)-3-oxo-24-norhopa-4(23),17(21)-diene (Figure 3 (24); Table 3, entry 24), 3-oxo-olean-12-ene-28,30-dioic acid (Figure 3 (25); Table 3, entry 25), β-amyrin (Figure 3 (26); Table 3, entry 26), and acteol-3-O-(2'-O-(E)-2-butenoyl)-β-D-xylopyranoside (Figure 3 (27); Table 3, entry 27) are also screened with 6LU7 which exhibit binding energies of −8.6, −8.5, −8.5, −8.3, −8.3, −8.2, −8.2, −8.2, −8.1, −8.1, −8.0, −7.6, −7.4, −7.2, −7.1, −6.8, and −6.7 kcal/mol, respectively. All types of saponins are isolated from many species of medicinal plants which are shown in Table 3. All saponins successfully dock with 6LU7 M^{pro} in our study, except for some minor violations. Further studies of these saponins against COVID-19 should be conducted in vitro and in vivo for validation.
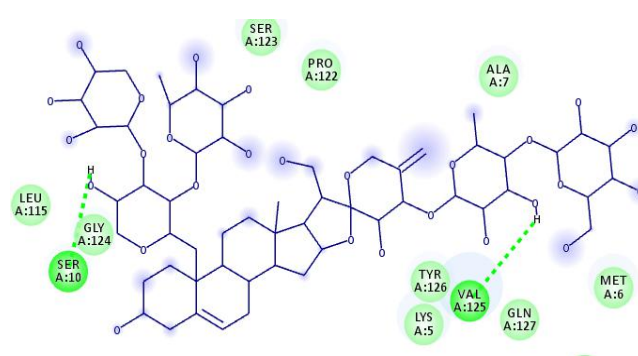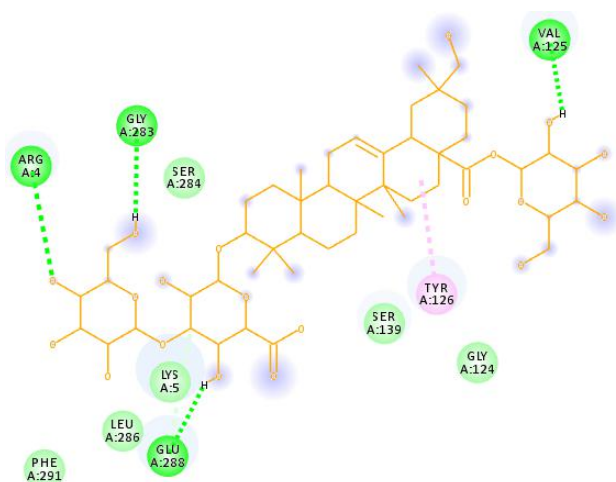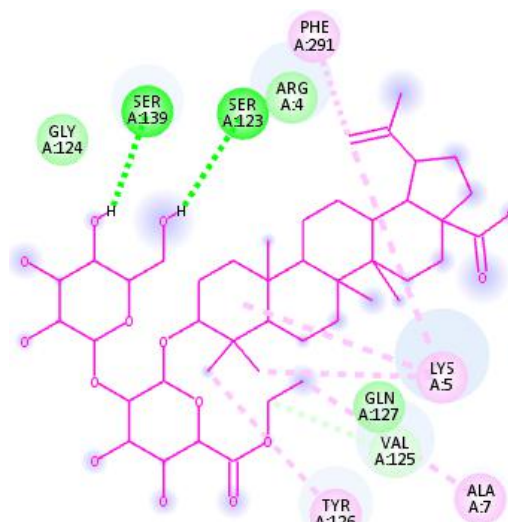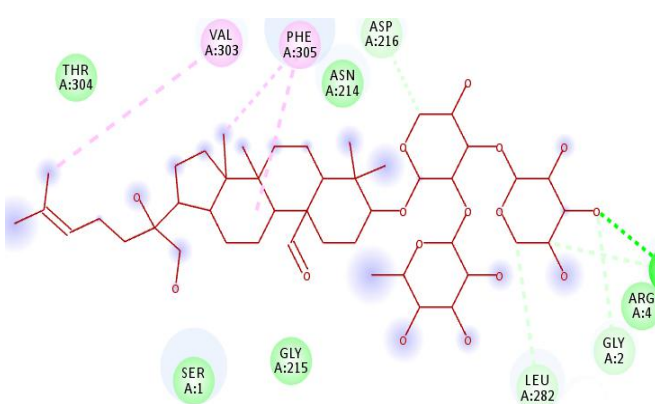

(1)

(2)
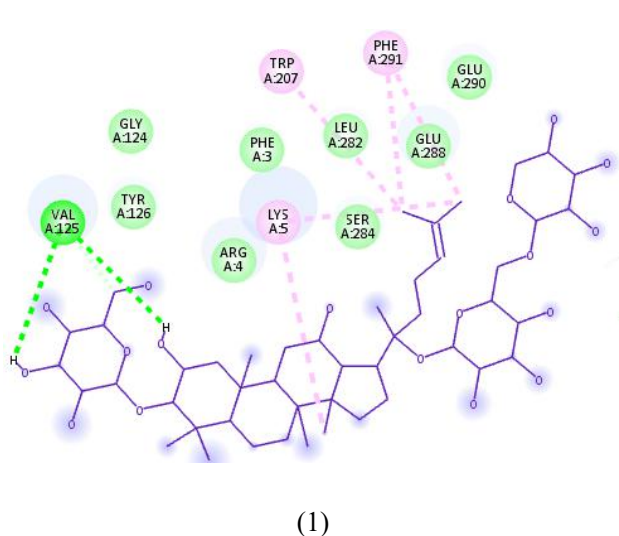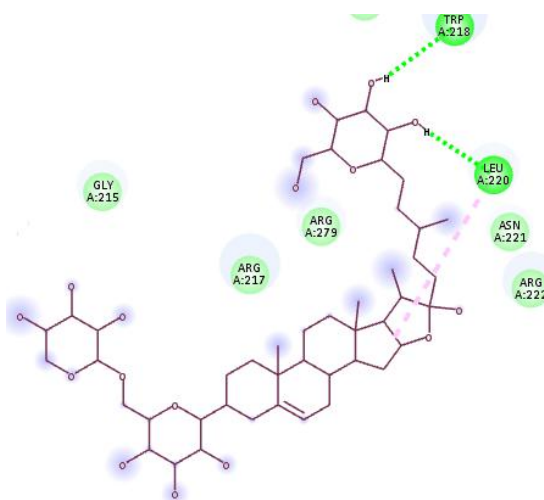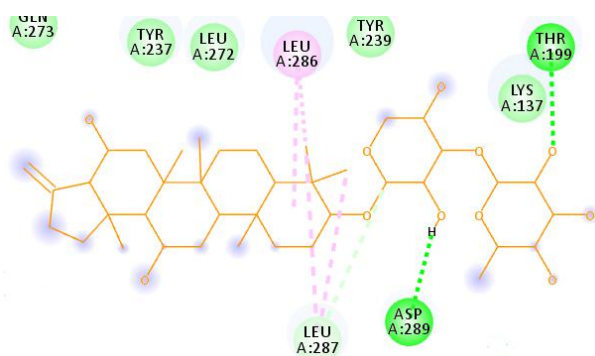
(3)

(4)

(5)

(6)

(7)
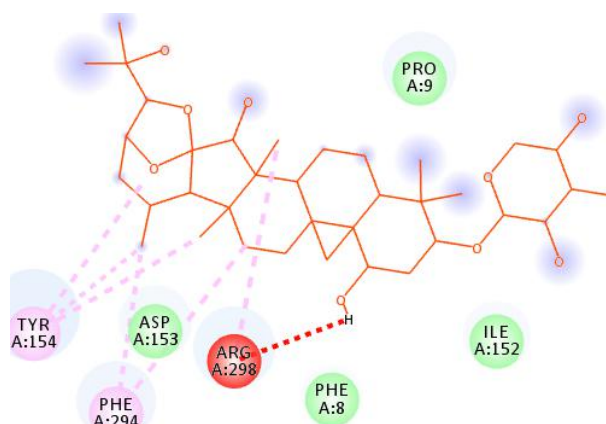
(8)
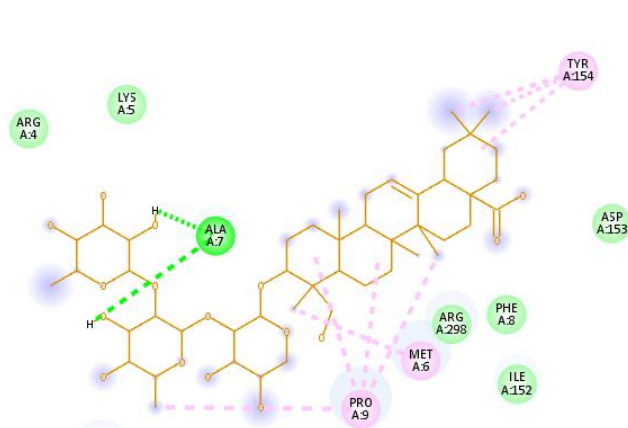
(9)
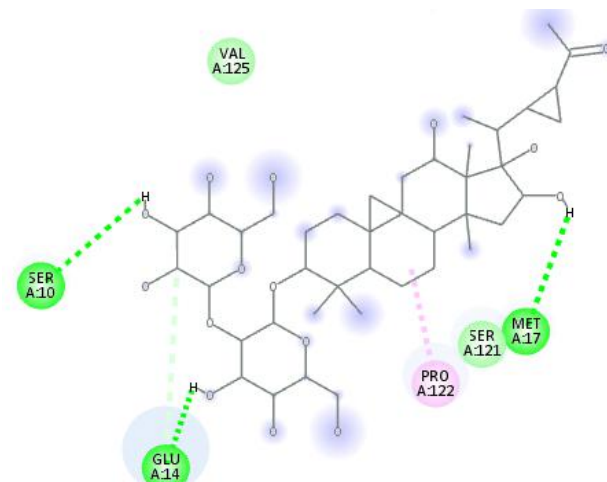
(10)
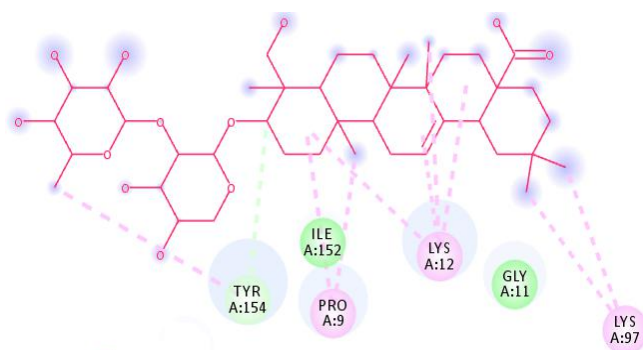
(11)
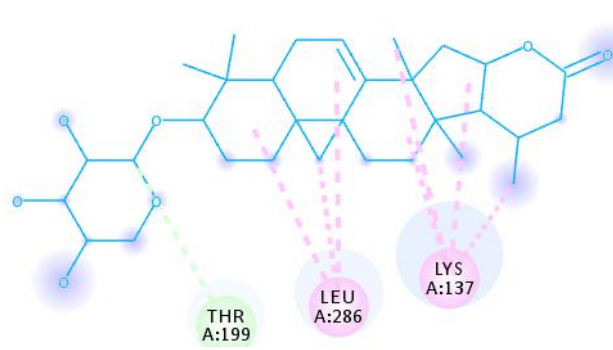
(12)

(13)

(14)

(15)

(16)

(17)

(18)

(19)

(20)

(21)

(22)

(23)

(24)

(25)

(26)

(27)
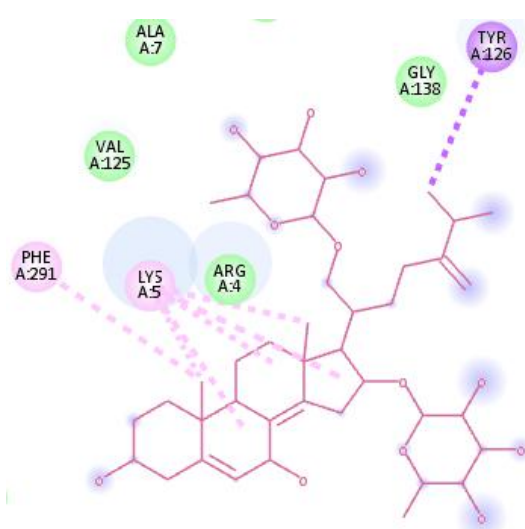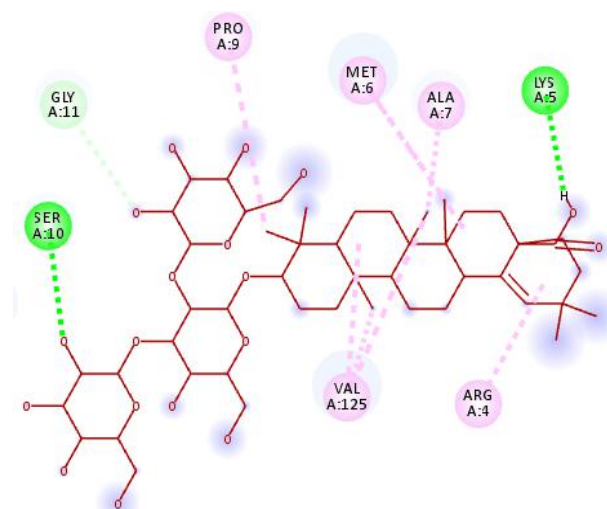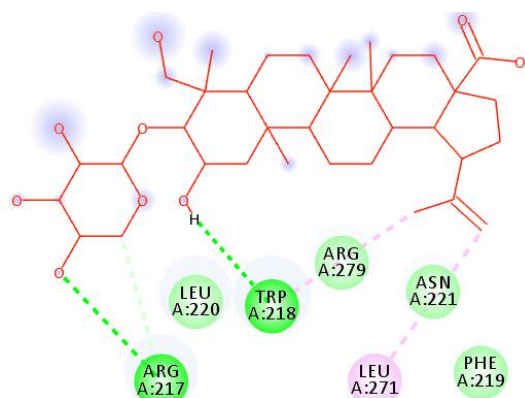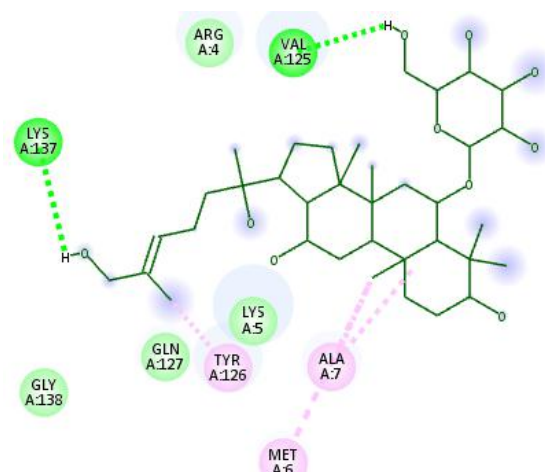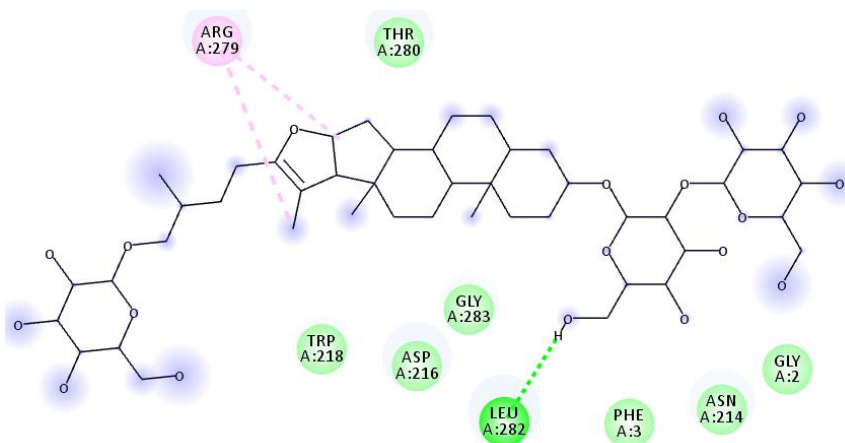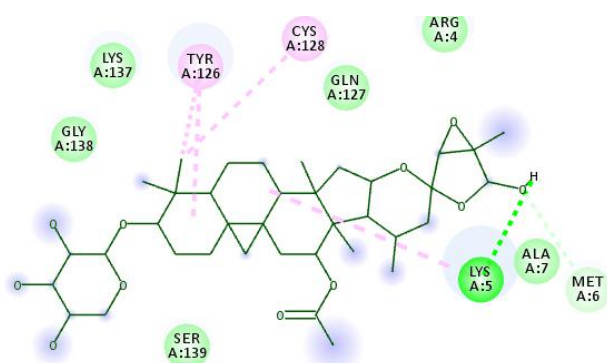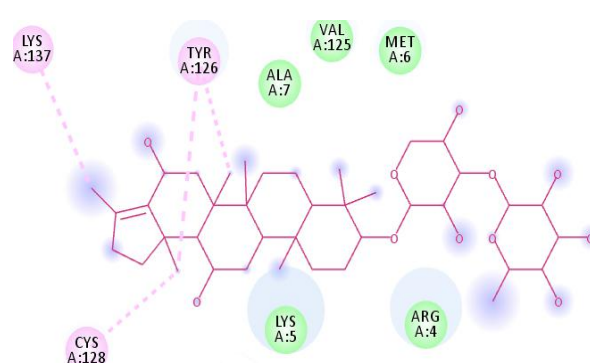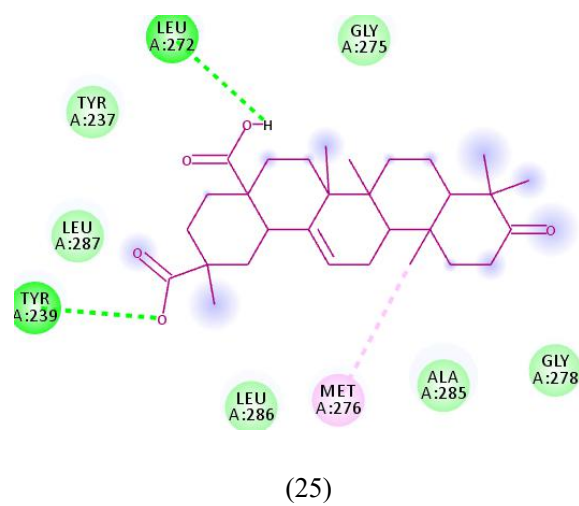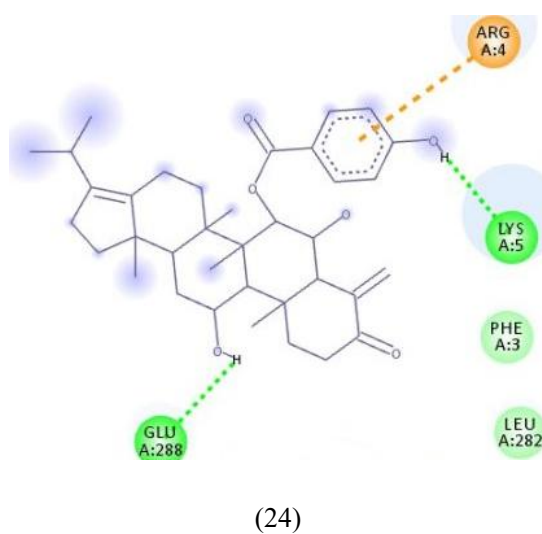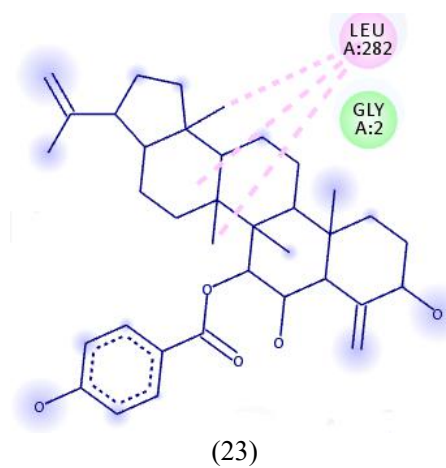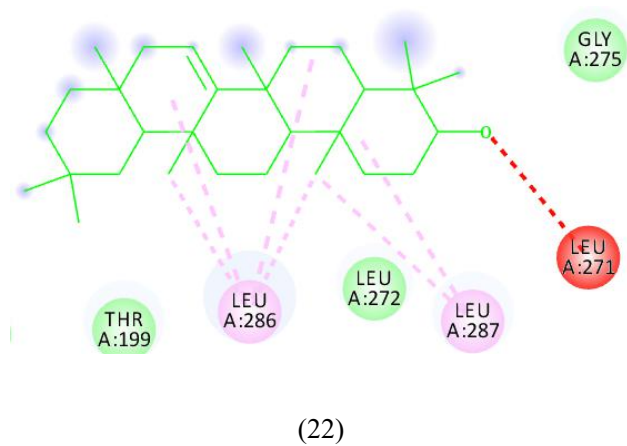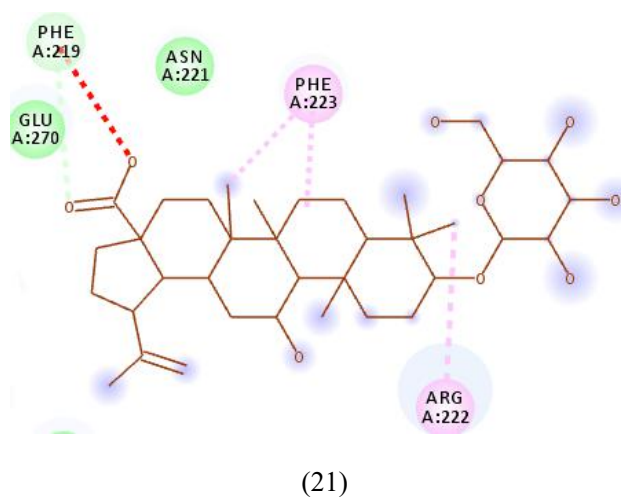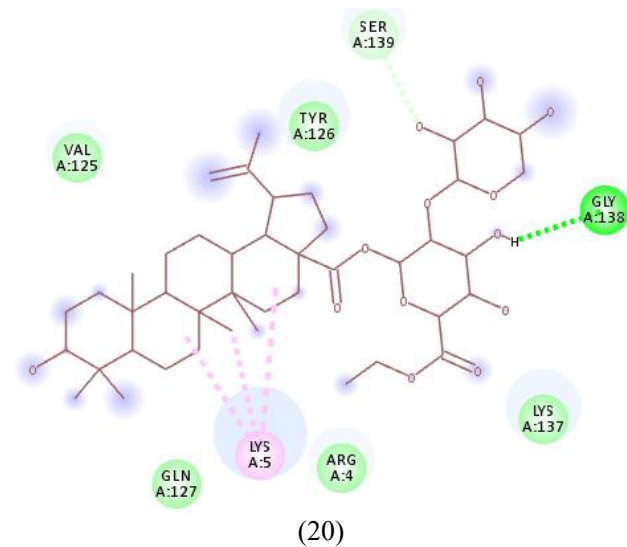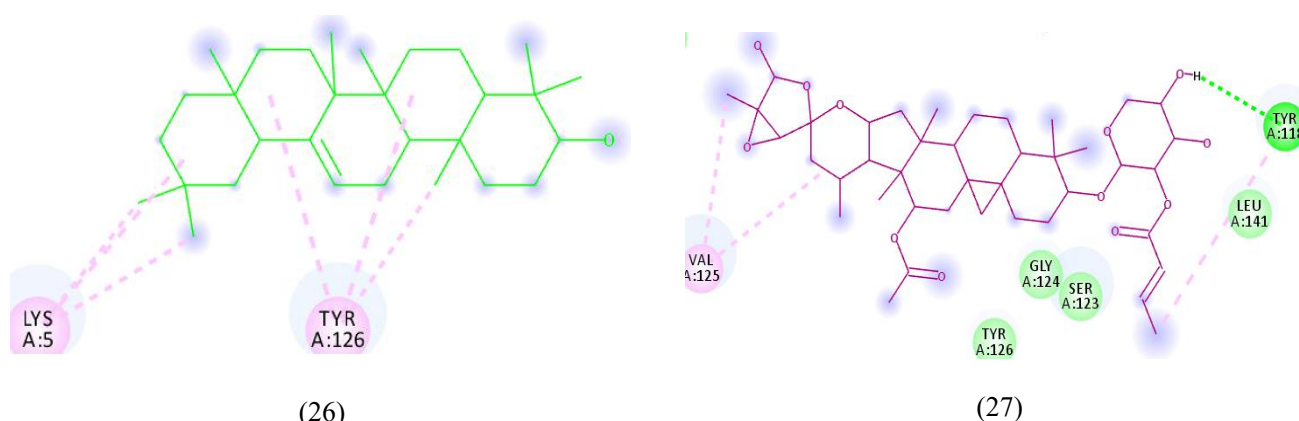
Figure 3 Molecular docking analysis of 6LU7 with several saponins. (1) gypenoside LVII, (2) smilscobinoside F, (3) glinusopposide L, (4) 25-O-acetylcimigenol-3-O-(3'-O-3-methoxy-3-oxopropionyl)-β-D-xylopyranoside, (5) calendustellatoside E, (6) schekwanglupaside A, (7) gylongiposide I, (8) (1S,15R)-1,15,25-trihydroxy-3-O-β-D-xylopyranosyl-acta-(16S,23R,24R)-16,23;16,24-binoxoside, (9) 3-O-α-L-arabinopyranosyl-(1S,24R)-1,24,25-trihydroxy-15-oxo-acta-(16R,23R)-16,23-monoxoside, (10) 9 (R), 19, 22 (S), 24 (R) dicyclolanost-3β, 12α, 16β, 17α tetrol-25-one 3-O-β-D-glucopyranosyl-(1→2)-β-D-glucopyranoside, (11) TPG3, (12) cimiheraclein G, (13) (20R)-16,21-O-di-(β-D-fucopyranosyl)-24-methyl-cholesta-5,24(28)-diene-3β,7α,16α,21-tetraol, (14) calendustellatoside D, (15) 2α,3β,23-trihydroxylup-20(29)-en-28-oic acid 3-O-α-L-arabinopyranoside, (16) yesanchinoside R₃, (17) anemarsaponin B, (18) actein, (19) glinusopposide M, (20) schekwanglupaside B, (21) 3-O-β-D-glucopyranosyl 3α, 11α-dihydroxylup-20(29)-en-28-oic acid, (22) taraxerol, (23) 3β,6β-dihydroxy-7β-((4-hydroxybenzoyl)oxy)-21αH-24-norhopa-4(23),22(29)-diene, (24) 6β,11α-dihydroxy-7β-((4-hydroxybenzoyl)oxy)-3-oxo-24-norhopa-4(23),17(21)-diene, (25) 3-oxo-olean-12-ene-28,30-dioic acid, (26) β-amyrin, and (27) acteol-3-O-(2'-O-(E)-2-butenoyl)-β-D-xylopyranoside.

Table 3 Binding energies and interaction of 27 saponins against coronavirus disease 2019 main protease
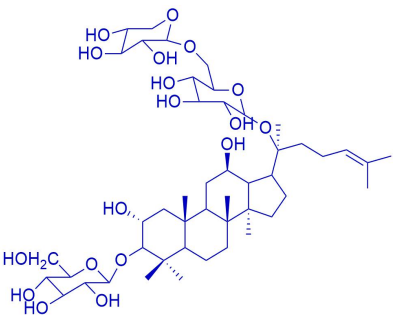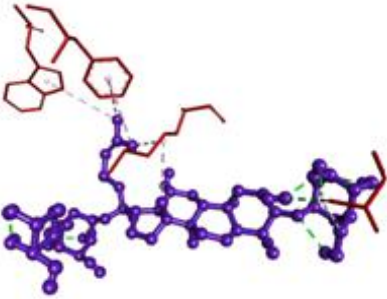
Entry	Structure/name	Interaction of structure with 4LU7	Docking affinity (kcal/mol)	Amino acid residue
1	Gypenoside LVII		−9.7	Val-125; Val-125; Lys-5; Trp-207; Phe-219

Table 3 Binding energies and interaction of 27 saponins against coronavirus disease 2019 main protease (*Continued*)
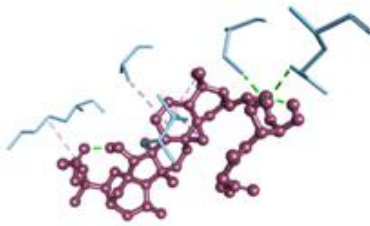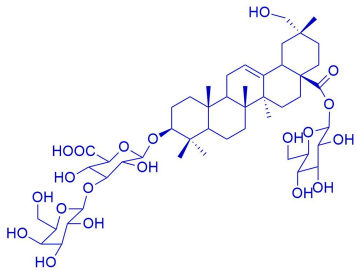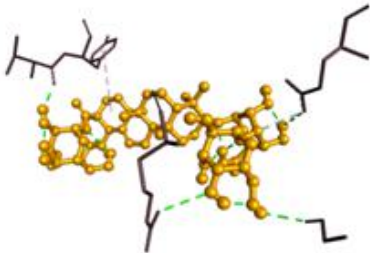
Entry	Structure/name	Interaction of structure with 4LU7	Docking affinity (kcal/mol)	Amino acid residue
2	Smilscobinoside F		−9.8	Trp-218; Leu-220; Leu-220
3	Glinusopposide L		−9.8	Thr-199; Asp-289; Leu-287; Leu-286
4	25-O-acetylcimigenol-3-O-[3'-O-3-methoxy-3-oxopropionyl]-β-D-xylopyranoside		−8.9	Ser-10; Glu-14; Lys-5; Ala-7; Val-125
5	Calendustellatoside E		−9.4	Arg-4; Val-125; Gly-283; Glu-288; Tyr-126

Table 3 Binding energies and interaction of 27 saponins against coronavirus disease 2019 main protease (*Continued*)
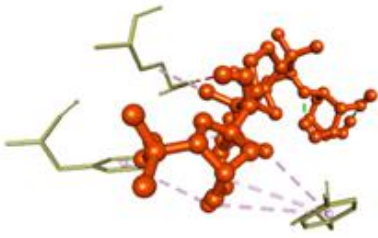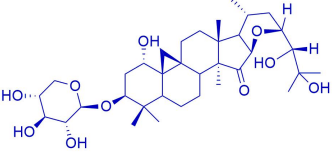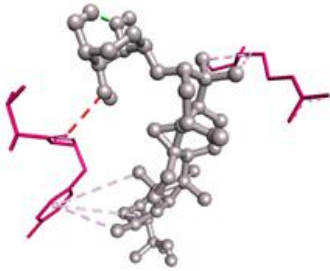
Entry	Structure/name	Interaction of structure with 4LU7	Docking affinity (kcal/mol)	Amino acid residue
6	Schekwanglupaside A		−9.1	Ser-123; Ser-139; Val-125; Lys-5; Ala-7; Tyr-126; Phe-291
7	Gylongiposide I		−8.9	Phe-3; Gly-2; Phe-3; Arg-4; Asp-216; Val-303; Phe-305
8	(1S,15R)-1,15,25-trihydroxy-3-O-β-D-xylopyranosyl-acta-(16S,23R,24R)-16,23;16,24-binoxoside		−8.8	Tyr-154; Phe-294; Arg-298
9	3-O-α-L-arabinopyranosyl-(1S,24R)-1,24,25-trihydroxy-15-oxo-acta-(16R,23R)-16,23-monoxoside		−8.8	Arg-4; Tyr-126

Table 3 Binding energies and interaction of 27 saponins against coronavirus disease 2019 main protease (*Continued*)
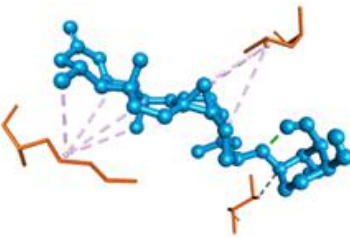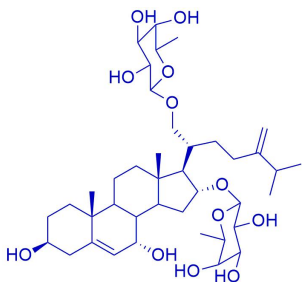
Entry	Structure/name	Interaction of structure with 4LU7	Docking affinity (kcal/mol)	Amino acid residue
10	9 (R), 19, 22 (S), 24 (R) dicyclolanost-3β, 12α, 16β, 17α tetrol-25-one3-O-β-D-glucopyran osyl-(1→2)-β-D-glucopyranoside		−8.6	Ser-10; Glu-14; Met-17; Pro-122
11	TPG3		−8.6	Tyr-154; Pro-9; Lys-12; Lys-97; Tyr-154;
12	Cimiheraclein G		−8.5	Lys-137; Thr-199; Leu-286
13	(20R)-16,21-O-di-(β-D-fucopyra nosyl)-24-methyl-cholesta-5,24(2 8)-diene-3β,7α,16α,21-tetraol		−8.5	Lyr-126; Lys-5; Phe-291

Table 3 Binding energies and interaction of 27 saponins against coronavirus disease 2019 main protease (*Continued*)
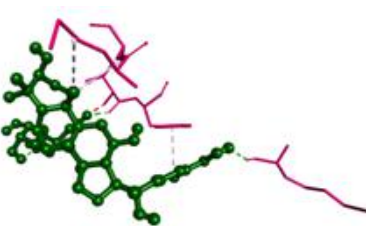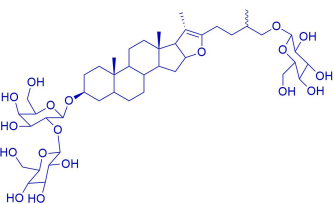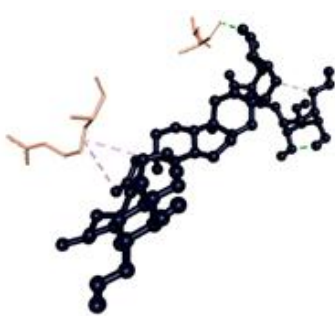
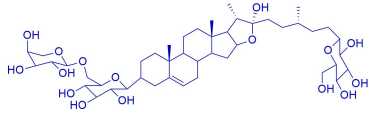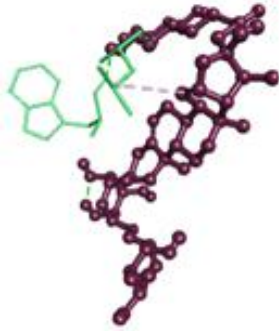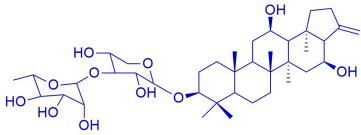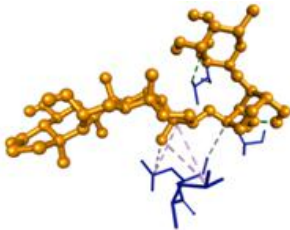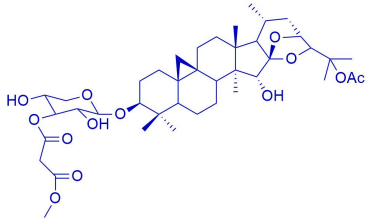| Entry	Structure/name	Interaction of structure with 4LU7	Docking affinity (kcal/mol)	Amino acid residue
14	Calendustellatoside D		−8.3	Lys-5; Ser-10; Gly-11; Arg-4; Pro-9; Met-6; Ala-7; Val-125
15	2α,3β,23-trihydroxylup-20(29)-en-28-oic acid 3-O-α-L-arabinopyranoside		−8.3	Arg-217; Trp-218; Arg-217; Leu-271; Trp-218
16	Yesanchinoside R$_3$		−8.2	Val-125; Lys-137; Met-6; Ala-7; Tyr-126
17	Anemarsaponin B		−8.2	Leu-282; Arg-279

Table 3 Binding energies and interaction of 27 saponins against coronavirus disease 2019 main protease (*Continued*)
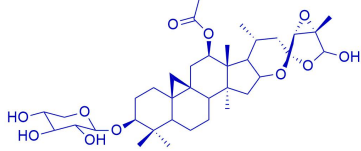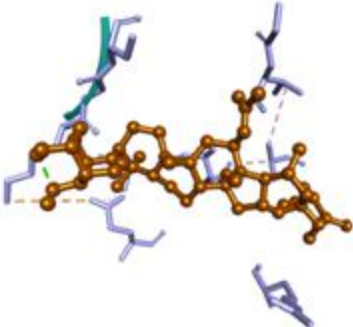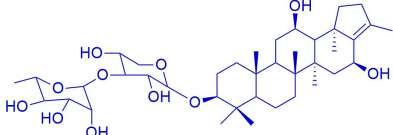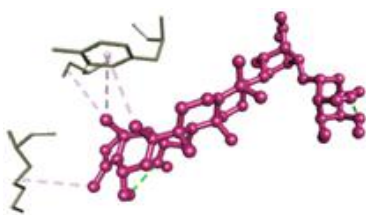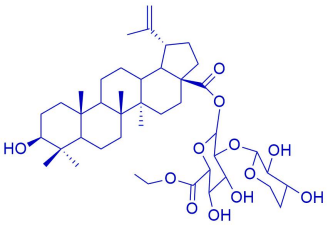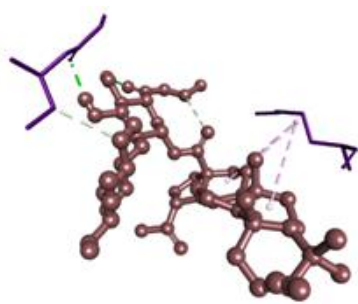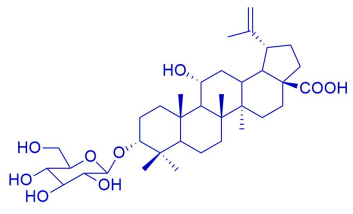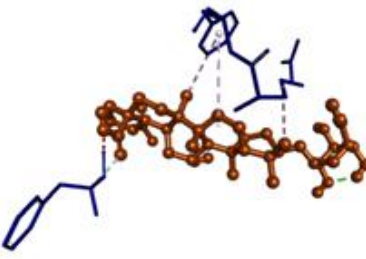
Entry	Structure/name	Interaction of structure with 4LU7	Docking affinity (kcal/mol)	Amino acid residue
18	Actein		−8.2	Lys-5; Met-6; Tyr-126; Cys-128; Lys-5
19	Glinusopposide M		−8.1	Tyr-126; Cys-128; Lys-137
20	Schekwanglupaside B		−8.1	Gly-138; Ser-139; Lys-5
21	3- O- β- D- glucopyranosyl 3α, 11α- dihydroxylup- 20(29)-en-28- oic acid		−8.0	Glu-270; Arg-222; Phe-223

Table 3 Binding energies and interaction of 27 saponins against coronavirus disease 2019 main protease (*Continued*)
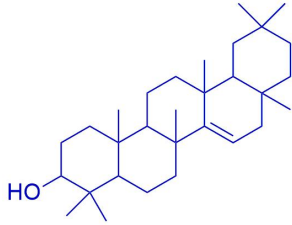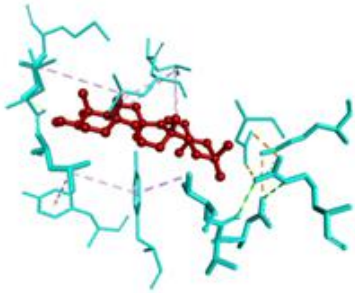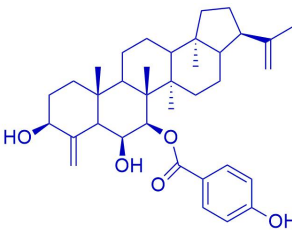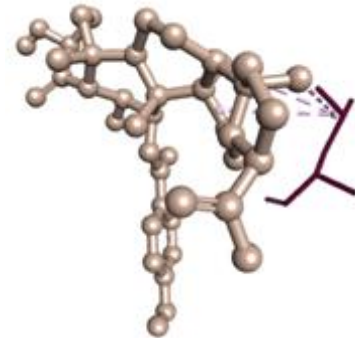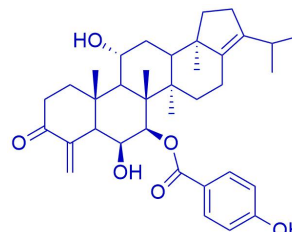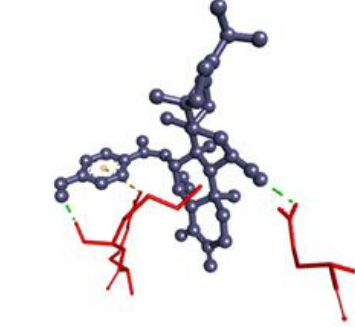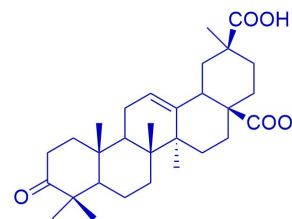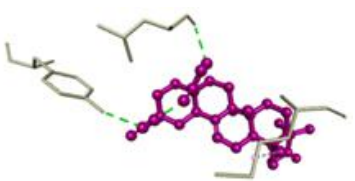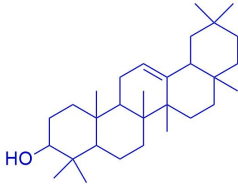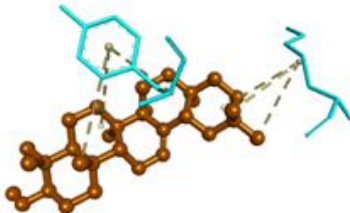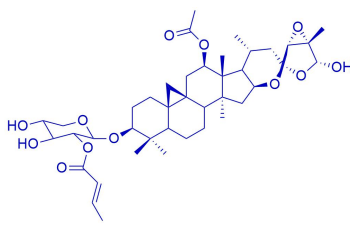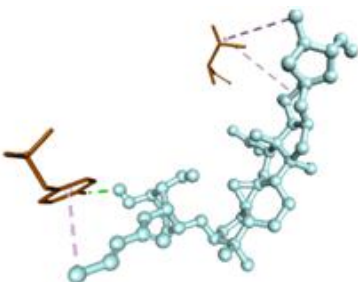
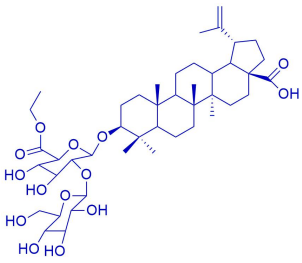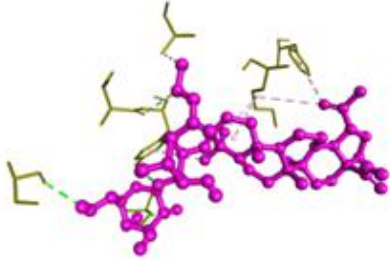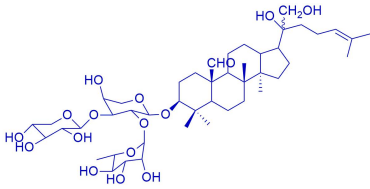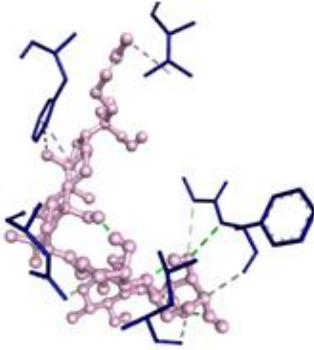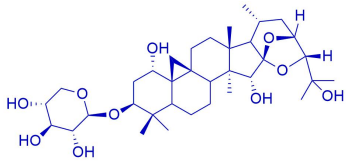| Entry	Structure/name	Interaction of structure with 4LU7	Docking affinity (kcal/mol)	Amino acid residue
22	Taraxerol		−7.6	Leu-286; Leu-287
23	3β,6β-dihydroxy-7β-((4-hydroxy benzoyl)oxy)-21αH-24-norhopa-4(23),22(29)-diene		−7.4	Leu-282
24	6β,11α-dihydroxy-7β-((4-hydrox ybenzoyl)oxy)-3-oxo-24-norhopa -4(23),17(21)-diene		−7.2	Arg-4; Lys-5; Glu-288
25	3-oxo-olean-12-ene-28,30-dioic acid		−7.1	Tyr-239; Leu-272; Met-276

Table 3 Binding energies and interaction of 27 saponins against coronavirus disease 2019 main protease (*Continued*)

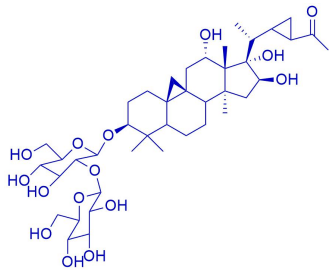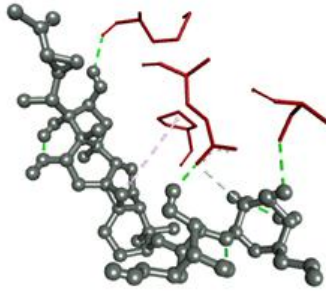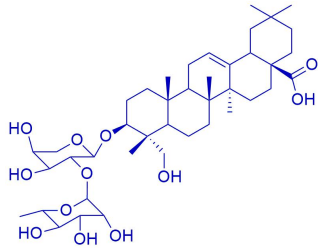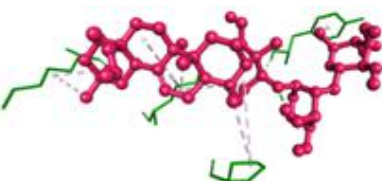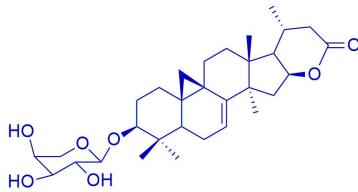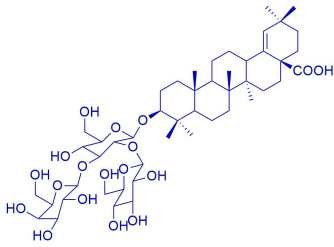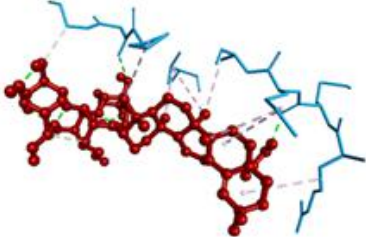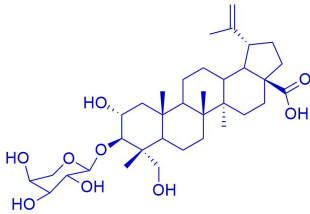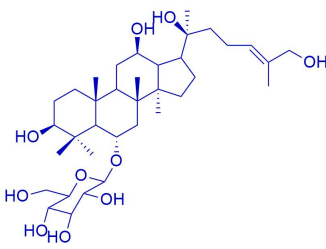| Entry	Structure/name	Interaction of structure with 4LU7	Docking affinity (kcal/mol)	Amino acid residue
26	β-amyrin		−6.8	Lys-5; Tyr-126
27	Acteol-3-O-(2'-O-(E)-2-butenoyl)-β-D-xylopyranoside		−6.7	Tyr-118; Val-125; Tyr-118

Discussion

Currently, the major threat to human health is the novel new SARS-CoV-2. There are no drugs available for the treatment of SARS-Cov-2-mediated infections. There is an urgent need for potent drugs for the treatment of coronavirus disease and stopping the dissemination of the virus [25–26]. We use diverse types of saponins against COVID-19 M^{pro} in silico.

Approximately, 34 diverse types of saponins were showing more binding affinity with COVID-19 M^{pro} than hydroxychloroquine, chloroquine, and nelfinavir, and their main original medical plant resources were shown in Table 4. 3-O-β-D-Xylopyranosyl-6-O-β-D-glucopyranosyl-16-O-β-D-glucopyranosyl-3β,6α,16β,24(S)-25-pentahydroxycycloartane is a cycloartane-type saponin found in *Astragalus brachycalyx* plant [30] (Table 4, entry 1). This saponin was showing an excellent binding affinity (−11.9 kcal/mol) with COVID-19 M^{pro}. Gypenoside J1 (Table 4, entry 7), gypenoside J2 (Table 4, entry 11), gypenoside J3 (Table 4, entry 12), and gypenoside LVII (Table 4, entry 14) are a dammarane-type saponin reported from *Gynostemma pentaphyllum* plant [35]. *Gynostemma pentaphyllum* plant is a big source of dammarane-type saponins, which showed an excellent binding affinity in the range from −10.4 to −9.7 kcal/mol. Schekwanglupaside A (Table 4, entry 19) and

schekwanglupaside B (Table 4, entry 33) are lupane-type saponins found in the *Schefflera kwangsiensis* plant which showed a moderate binding affinity in the range from −9.1 to −8.1 kcal/mol [42]. Saponins are very important for human life which play a vital role in diverse biological activities.

Actein (Table 4, entry 31) is a cycloartane saponin which exhibited anticancer activities on MCF-7, SW-480, SMMC-7721, A-549, and HL-60 human cancer cell lines and is found in rhizomes of *Cimicifuga foetida* [27]. The interaction of this saponin displayed binding affinity −8.2 kcal/mol with COVID-19 M^{pro}. *Panax ginseng* is a useful plant that has been used in hypotensive, antioxidant, sedative, analgesic, and endocrine activities. Ginsenoside Rg12 (Table 4, entry 2) is isolated from the root of this plant [28]. This saponin displayed excellent binding affinity −10.9 kcal/mol with COVID-19 M^{pro}. *Acanthopanax gracilistylus* plant has been used in the treatment of many diseases such as bone pains, liver disease, arthritis, and paralysis [29]. Acankoreoside A (Table 4, entry 6) was reported from this plant which displayed the best binding affinity −10.5 kcal/mol with COVID-19 M^{pro}. Thirteen highly potential saponins (binding affinity above −10 kcal/mol) in this study may show a better outcome in COVID-19. This method presented here can play a highly potential role in rapid drug discovery with a clinical trial against the COVID-19.

Table 4 Isolation of saponins from species of medicinal plant

Entry	Saponins	Type	(Genus/species Chinese name) scientific name/parts	Reference
1	3-O-β-D-Xylopyranosyl-6-O-β-D-glucopyranosyl-16-O-β-D-glucopyranosyl-3β,6α,16β,24(S)-25-pentahydroxy cycloartane	Cycloartane	*Astragalus brachycalyx*/roots	[30]
2	Ginsenoside Rg12	Dammarane	Renshen (*Panax ginseng*)/roots	[28]
3	TPG1	Oleanane	Citongcao (*Trevesia palmate*)/leaves	[31]
4	(23S,24S)-21-Hydroxymethyl-24-{[O-β-d-glucopyranosyl-(1→4)-β-dfucop-yranosyl]oxy}-3β,23-dihydroxyspirosta-5,25(27)-diene-1β-yl O-(α-L-rhamnopyranosyl)-(1→2)-O-[β-d-xylopyranosyl-(1→3)-α-L-arabinopyranoside	Steroid	Tiekuaizi (*Helleborus thibetanus*)/roots and rhizomes	[32]
5	3β-O-(α-L-Rhamnopyranosyl-(1→2)-β-D-glucopyranosyl-(1→2)-β-D-glucuronopyranosyl) betulinic acid 28-O-(α-L-rhamnopyranosyl-(1→4)-β-D-glucopyranoside)	Lupane	Baihuaezhangchai (*Schefflera kwangsiensis*)/aerial parts	[33]
6	Acankoreoside A	Lupane	Wujia (*Acanthopanax gracilistylus*)/leaves	[34]
7	Gypenoside J1	Dammarane	Jiaogulan (*Gynostemma pentaphyllum*)/aerial parts	[35]
8	Paristenoside B	Spirostanol	Chong Lou (*Paris polyphylla*)/rhizomes	[36]
9	TPG2	Oleanane	*Trevesia palmate*/leaves	[31]
10	Cyclocarioside Q	Dammarane	Qingqianliu (*Cyclocarya paliurus*)/leaves	[37]
11	Gypenoside J2	Dammarane	Jiaogulan (*Gynostemma pentaphyllum*)/aerial parts	[35]
12	Gypenoside J3	Dammarane	*Gynostemma pentaphyllum*/aerial parts	[35]
13	Paristenoside A	Spirostanol	Qiyeyizhihua (*Paris polyphylla*)/rhizomes	[36]
14	Gypenoside LVII	Dammarane	*Gynostemma pentaphyllum*/aerial parts	[35]
15	Smilscobinoside F	Steroid	Duangengbaqia (*Smilax scobinicaulis*)/rhizomes	[38]

Table 4 Isolation of saponins from species of medicinal plant (*Continued*)

Entry	Saponins	Type	(Genus/species Chinese name) scientific name/parts	Reference
16	Glinusopposide L	Hopane	Jiafanlu (*Glinus oppositifolius*)/whole plant	[39]
17	25-O-Acetylcimigenol-3-O-(3'-O-3-methoxy-3-oxopropionyl)-β-D-xylopyranoside	Cycloartane	Shengma (*Cimicifuga foetida*)/rhizomes	[40]
18	Calendustellatoside E	Oleanane	Jinzhanhuashu (*Calendula stellata*)/whole plant	[41]
19	Schekwanglupaside A	Lupane	*Schefflera kwangsiensis*/aerial parts	[42]
20	Gylongiposide I	Dammarane	*Gynostemma pentaphyllum*/aerial parts	[43]
21	(1S,15R)-1,15,25-Trihydroxy-3-O-β-D-xylopyranosyl-acta-(16S,23R,24R)-16,23;16,24-binoxoside	Cycloartane	Leiyeshengmashu (*Actaea racemosa*)/aerial parts	[44]
22	3-O-α-L-Arabinopyranosyl-(1S,24R)-1,24,25-trihydroxy-15-oxo-acta-(16R,23R)-16,23-monoxoside	Cycloartane	*Actaea racemosa*/aerial parts	[44]
23	9 (R), 19, 22 (S), 24 (R) Dicyclolanost-3β, 12α, 16β, 17α tetrol-25-one 3-O-β-D-glucopyranosyl-(1→2)-β-D-glucopyranoside	Cycloartane	*Mussaenda luteola*/aerial parts	[45]
24	TPG3	Oleanane	*Trevesia palmate*/leaves	[31]
25	Cimiheraclein G	Cycloartane	Dasanyeshengma (*Actaea heracleifolia*)/aerial parts (Li pi lu haixing)	[46]
26	Granulatoside C	Steroid	*Choriaster granulatus*/starfish	[47]
27	Calendustellatoside D	Oleanane	*Calendula stellata*/whole plant	[41]
28	2α,3β,23-Trihydroxylup-20(29)-en-28-oic acid 3-O-α-L-arabinopyranoside	Lupane	*Trevesia palmate*/leaves	[48]
29	Yesanchinoside R3	Dammarane	Zhujieshen (*Panax japonicus*)/rhizomes	[49]
30	Anemarsaponin B	Steroid	Zhimu (*Anemarrhena asphodeloides*)/rhizome	[50]
31	Actein	Cycloartane	*Cimicifuga foetida*/rhizome	[40]

Table 4 Isolation of saponins from species of medicinal plant (*Continued*)

Entry	Saponins	Type	(Genus/species Chinese name) scientific name/parts	Reference
32	Glinusopposide M	Hopane	*Glinus oppositifolius*/whole plant	[39]
33	Schekwanglupaside B	Lupane	*Schefflera kwangsiensis*/aerial parts	[42]
34	3- O- β- D- Glucopyranosyl 3α, 11α- dihydroxylup- 20(29)- en- 28- oic acid	Lupane	Wujia (*Acanthopanax gracilistylus*)/leaves	[34]
35	taraxerol	Oleanane	Shiwancuoshu (*Asystasia buettneri*)/aerial parts	[51]
36	3β,6β-Dihydroxy-7β-((4-hydroxybenzoyl)oxy)-21αH-24-norhopa-4(23),22(29)-diene	Hopane	*Zanha africana*/root bark	[52]
37	6β,11α-Dihydroxy-7β-((4-hydroxybenzoyl)oxy)-3-oxo-24-norhopa-4(23),17(21)-diene	Hopane	*Zanha africana*/root bark	[52]
38	3-Oxo-olean-12-ene-28,30-dioic acid	Hopane	Jiafulu (*Glinus oppositifolius*)/whole plant	[39]
39	β-Amyrin	Oleanane	Mumian (*Bombax ceiba*)/leaves	[53]
40	Acteol-3-O-(2'-O-(E)-2-butenoyl)-β-D-xylopyranoside	Cycloartane	Shengma (*Cimicifuga foetida*)/rhizome	[40]

Conclusion

COVID-19 is a major challenge for the global health sector. Currently, there is no approved drug for the treatment of the disease. In the present time, the available drugs act on the Mpro for the treatment of COVID-19. In this study, we examine various saponins, which may be useful for the treatment of COVID-19. Approximately, 34 diverse types of saponins were showing more binding affinity with COVID-19 Mpro than hydroxychloroquine, chloroquine, and nelfinavir and may act as COVID-19 Mpro inhibitors, among which 13 highly potential saponins have binding affinity above −10 kcal/mol. So, further research on medicinal plant-derived saponins and plant extract is necessary for the treatment of COVID-19.

References

1. Huang C, Wang Y, Li X, et al. Clinical features of patients infected with 2019 novel coronavirus in Wuhan China. *Lancet*. 2020;395(10223): 497–506.

2. Coronaviridae Study Group of the International Committee on Taxonomy of Viruses. The species Severe acute respiratory syndrome-related coronavirus: classifying 2019-nCoV and naming it SARS-CoV-2. *Nat Microbiol*. 2020;5(4): 536–544.

3. Chang D, Lin M, Wei L, Xie L, Zhu G. Epidemiologic and clinical characteristics of novel coronavirus infections involving 13 patients outside Wuhan China. *JAMA*. 2020;323(11): 1092–1093.

4. World Health Organization. Coronavirus disease 2019 (COVID-19). Situation Report. https://www.who.int/docs/default-source/coronaviruse/situation-reports/20200708-covid-19-sitrep-170.pdf?sfvrsn=bca86036_2. Accessed July 8, 2020.

5. Lu H. Drug treatment options for the 2019-new coronavirus (2019-nCoV). *Biosci Trends*. 2020;14(1):69–71.

6. Lu R, Zhao X, Li J, et al. Genomic characterisation and epidemiology of 2019 novel coronavirus: implications for virus origins and receptor binding. *Lancet*. 2020;395(10224):

565–574.

7. Jin Z, Du X, Xu Y, et al. Structure of M^pro from COVID-19 virus and discovery of its inhibitors. *bioRxiv*. 2020;02(26):964882.

8. Chauhan A, Kalra S. Identification of potent COVID-19 main protease (MPRO) inhibitors from flavonoids. *Res Square*. 2020. https://doi.org/10.21203/rs.3.rs-34497/v1. Accessed July 8, 2020.

9. Sekiou O, Bouziane I, Bouslama Z, Djemel A. In-silico identification of potent inhibitors of COVID-19 main protease (M^pro) and Angiotensin converting enzyme 2 (ACE2) from natural products: Quercetin, Hispidulin, and Cirsimaritin exhibited better potential inhibition than Hydroxy-Chloroquine against COVID-19 main protease active site and ACE2. *ChemRxiv*. 2020. https://doi.org/10.26434/chemrxiv.12181404.v1. Accessed July 8, 2020.

10. Zhang L, Lin D, Sun X, et al. Crystal structure of SARS-CoV-2 main protease provides a basis for design of improved a-ketoamide inhibitors. *Science*. 2020;368(6489):409–412.

11. Rehan M, Shafiullah, Mir SA. Structural diversity, natural sources, and pharmacological potential of plant-based saponins with special focus on anticancer activity: a review. *Med Chem Res*. 2020;29:1707–1722.

12. Patwardhan B, Warude D, Pushpangadan P, Bhatt N. Ayurveda and traditional Chinese medicine: a comparative overview. *Evid Based Complement Alternat Med*. 2005;2(4):465–473.

13. Kabir H. Introduction to Ilmul Advia. Aligarh: Shamsher Publishers and Distributors, 2002.

14. Nair R, Sellaturay S, Sriprasad S. The history of ginseng in the management of erectile dysfunction in ancient China (3500–2600 BCE). *Indian J Urol*. 2012;28(1):15–20.

15. Cheng JG. Investigation of the plant Jiaogulan and its analogous herb, Wulianmei. *Zhong Cao Yao*. 1990;21(9):424.

16. Papadopoulou K, Melton RE, Leggett M, Daniels MJ, Osbourn AE. Compromised disease resistance in saponin-deficient plants. *PNAS*. 1999;96(22):12923–12928.

17. Ito M, Nakashima H, Baba M, Pauwels R, De Clercq E, Shigeta S. Inhibitory effect of glycyrrhizin on the in vitro inefectivity and cytopathic activity of the human immunodeficienccy virus [HIV (HTLV-III/LAV)]. *Antiviral Res*. 1986;7(3):127–137.

18. Roner MR, Tam KI, Kiesling-Barrager M. Prevention of rotavirus infections in vitro with aqueous extractions of Quillaja Saponaria Molina. *Future Med Chem*. 2010;2(7):1083–1097.

19. Adams MM, Damani P, Perl NR, et al. Design and synthesis of potent Quillaia saponin vaccine adjuvants. *J Am Chem Soc*. 2010;132(6):1–16.

20. Bomford R. The comparative selectivity of adjuvants for humoral and cell-mediated immunity. *Clin Exp Immunol*. 1980;39:426–434.

21. Rajput ZI, Hu SH, Xiao CW, Arijo AG. Adjuvant effects of saponins on animal immune responses. *J Zhejiang Univ Sci B*. 2006;8(3):153–161.

22. Murgueitio MS, Bermudez M, Mortier J, Wolber G. In silico virtual screening approaches for anti-viral drug discovery. *Drug Discov Today Technol*. 2012;9(3):e219–225.

23. Burley SK, Berman HM, Kleywegt GJ, Markley JL, Nakamura H, Velankar S. Protein Data Bank (PDB): the single global macromolecular structure archive. *Methods Mol Biol*. 2017;1607:627–641.

24. Cortegiani A, Ingoglia G, Ippolito M, Giarratano A, Einav S. A systematic review on the efficacy and safety of chloroquine for the treatment of COVID-19. *J Crit Care*. 2020;57:279–283.

25. Zhu N, Zhang D, Wang W, et al. A novel coronavirus from patients with pneumonia in China, 2019. *N Engl J Med*. 2020;382:727–733.

26. Zhou Y, Hou Y, Shen J, Huang Y, Martin W, Cheng F. Network-based drug repurposing for novel coronavirus 2019-nCoV/SARS-CoV-2. *Cell Discov*. 2020;6:14.

27. Ahmad VU, Mohammad FV, Tareen RB. Laceioside, a new cycloartane saponin from *Astragalus tephrosioides Boiss. var. lacei (Ali) Kirchoff*. *Nat Prod Res*. 2019;33(3):393.

28. Lee DG, Lee J, Cho I-H, et al. Ginsenoside Rg12, a new dammarane-type triterpene saponin from *Panax ginseng* root. *J Ginseng Res*. 2017;41(4):531–533.

29. Zou QP, Liu XQ, Huang JJ, et al. Inhibitory effects of lupane-type triterpenoid saponins from the leaves of *Acanthopanax gracilistylus* on lipopolysaccharide-induced TNF-α, IL-1β and high-mobility group box 1 release in macrophages. *Mol Med Rep*. 2017;16(6):9149–9156.

30. Aslanipour B, Gülcemal D, Nalbantsoy A, Yusufoglu H, Bedir E. Cycloartane-type glycosides from *Astragalus brachycalyx fischer* and their effects on cytokine release and hemolysis. *Phytochem Lett*. 2017;21:66–73.

31. Kim B, Han JW, Ngo MT, et al. Identification of novel compounds, oleanane- and ursane-type triterpene glycosides, from *Trevesia palmata*: their biocontrol activity against phytopathogenic fungi. *Sci Rep*. 2018;8(1):14522.

32. Zhang H, Su YF, Yang FY. Three new steroidal saponins from *Helleborus thibetanus*. *Nat Prod Res*. 2016;30(15):1724–1730.

33. Wang Y, Zhang CL, Liu YF, Chen RY, Wang FZ, Yu DQ. Two new lupane saponins from *Schefflera kwangsiensis*. *Phytochem Let*. 2016;18:19–22.

34. Zou QP, Liu XQ, Huang JJ, et al. Inhibitory

effects of lupane‑type triterpenoid saponins from the leaves of *Acanthopanax gracilistylus* on lipopolysaccharide‑induced TNF‑ α, IL‑1β and high‑mobility group box 1 release in macrophages. *Mol Med Rep*. 2017;16(6):9149–9156.

35. Xiang L, Zhang L, Chen X, Xia X, Li R, Zhong J. Ursane-type triterpenoid saponins from *Elsholtzia bodinieri*. *Nat Prod Res*. 2019;33(9):1349–1356.

36. Jin LY, Lu TX, Qin XJ, et al. Two new highly oxygenated spirostanol saponins from *paris polyphylla* var. stenophylla. *Nat Prod Bioprospect*. 2016;6(4):205–210.

37. Wang YR, Cui BS, Han SW, Li S. New dammarane triterpenoid saponins from the leaves of *Cyclocarya paliurus*. J *Asian Nat Prod Res*. 2018;20(11):1019–1027.

38. Shu J, Zhu G, Huang G, et al. New steroidal saponins with L-arabinose moiety from the rhizomes of *Smilax scobinicaulis*. *Phytochem Lett*. 2017;21:194–199.

39. Zhang D, Fu Y, Yang J, et al. Triterpenoids and their glycosides from *Glinus oppositifolius* with antifungal activities against *Microsporum gypseum* and *Trichophyton rubrum*. *Molecules*. 2019; 24(12): 2206.

40. Lu J, Peng XR, Li DS, Shi QQ, Qiu MH. Cytotoxic cycloartane triterpenoid saponins from the rhizomes of *Cimicifuga foetida*. *Nat Prod Bioprosp*. 2019;9(4):303–310.

41. Lehbili M, Magid AA, Kabouche A, et al. Oleanane-type triterpene saponins from *Calendula stellata*. *Phytochemistry*. 2017;144:33–42.

42. Wang Y, Zhang CL, Liu YF, Chen RY, Wang FZ, Yu DQ. Two new lupane saponins from *Schefflera kwangsiensis*. *Phytochem Lett*. 2016;18:19–22.

43. Lundqvist LCE, Rattigan D, Ehtesham E, Demmou C, Östenson CG, Sandström C. Profiling and activity screening of Dammarane-type triterpen saponins from *Gynostemma pentaphyllum* with glucosedependent insulin secretory activity. *Sci Rep*. 2018;9(1):627.

44. Imai A, Lankin DC, Nikolic D, et al. Cycloartane triterpenes from the aerial parts of *Actaea racemosa*. *J Nat Prod*. 2016;79(3):541–554.

45. Mohamed SM, Backheet EY, Bayoumi SA, Rossa SA. New cycloartane saponin and monoterpenoid glucoindole alkaloids from *Mussaenda luteola*. *Fitoterapia*. 2016;110:129–134.

46. Shi QQ, Wang WH, Lu J, Li DS, Zhou L, Qui MH. New cytotoxic cycloartane triterpenes from the aerial parts of *Actaea heracleifolia* (syn. *Cimicifuga heracleifolia*). *Planta Med*. 2019;85(2):154–159.

47. Ivanchina NV, Malyarenko TV, Kicha AA, Kalinovsky AI, Dmitrenoka PS, Stonik VA. A new steroidal glycoside granulatoside C from the starfish *Choriaster granulatus*, unexpectedly combining structural featuresof polar steroids from several different marine invertebrate phyla. *Nat Prod Commun*. 2017;12:1585–1588.

48. Yen PH, Doan VV, KimLien GT, et al. New lupane-type and ursane-type triterpene saponins from the leaves of *Trevesia palmate*. *Nat Prod Res*. 2019;1–8.

49. Zhu TF, Deng QH, Li P, Hu LF, Yan ZH, Yang YJ. A new dammarane-type saponin from the rhizomes of *Panax japonicas*. *Chem Nat Comp*. 2018;54:4.

50. Yang BY, Zhang J, Liu Y, Kuang HX. Steroidal saponins from the rhizomes of *Anemarrhena asphodeloides*. *Molecules*. 2016;21(8):1075.

51. Hamid AA, Aiyelaagbe OO, Negic AS, Luqman S, Kaneez F. Isolation and antiproliferative activity of chemical constituents from *Asystasia buettneri* Lindau. *Nat Prod Res*. 2018;32(17):2076–2080.

52. Stevenson PC, WC Green P, Veitch NC, Farrell IW, Kusolwa P, Belmain SR. Nor-hopanes from *Zanha africana* root bark with toxicity to bruchid beetles. *Phytochemistry*. 2016;123:25–32.

53. Mostafa NM. β-Amyrin rich *Bombax ceiba* leaf extract with potential neuroprotective activity against scopolamine-induced memory impairment in rats. *Rec Nat Prod*. 2018;12(5):480–492.